UNIVERSITAT POLITÈCNICA DE CATALUNYA
BARCELONATECH

telecos BCN

Study of selective contacts of electrons for tandem solar cells

---

A Degree Thesis

Submitted to the Faculty of the

Escola Tècnica d'Enginyeria de Telecomunicació de Barcelona

Universitat Politècnica de Catalunya

by

ALBERT POBLADOR BONET

In partial fulfilment

of the requirements for the degree in

Telecommunications Technologies and Services **ENGINEERING**

Advisors: PABLO RAFAEL ORTEGA VILLASCLARAS

GERARD MASMITJÀ RUSIÑOL

Barcelona, February 2021

Abstract

Humanity has faced a variety of problems throughout its history. From wars and conflicts to pandemics and famine. Today, one of the biggest problems we have as a society is climate change that is dragging us into global warming. Alternatives to fossil fuels are becoming more popular, especially solar energy. In this dissertation we will discuss one of their biggest limitations.

Tandem solar cells are an innovative technology that allows us to join two or more solar cells with different light spectrum absorption properties and thus be able to increase the efficiency of the total system. Joining the cells is not an easy task, as the binding nexus must be as efficient as possible.

In this project, we designed the intermediate layer using ITO (and Ag when we needed for making measurements) on an ETL (Electron Transport Layer) formed mainly by a phosphorus diffusion region on crystalline silicon substrates. Later, we studied two of the parameters that could most affect our efficiency.

One of the parameters was the series resistance, as we are interested in the intermediate layer being as least resistive as possible to avoid ohmic losses. On the other hand, we have studied cell passivation in order to know the recombinant losses of the cell surface.

After the experiments carried out, we observed that our results are good at relatively low temperatures (0 - 200 ° C), allowing us to manufacture tandem structures under these conditions. However, for high temperatures, the results are not good enough and although experiments were carried out to try to correct the degradation with temperature, we did not achieve an adequate result for higher temperatures.

Resum

La humanitat ha hagut de confrontar diversitat de problemes durant la seva història. Des de guerres i conflictes fins a pandèmies i fam. Avui dia, un dels problemes més grans que tenim com a societat és el canvi climàtic que ens està arrossegant a un escalfament global. Les alternatives als combustibles fòssils estan popularitzant-se, destacant per sobre de totes l'energia solar. En aquest document tractarem una de les seves limitacions tecnològiques més grans.

Les cel·les solars tàndem son una innovadora tecnologia que ens permet unir dues o més cel·les solars amb diferents propietats d'absorció de l'espectre de llum i així poder augmentar l'eficiència del sistema total. Unir les cel·les és una tasca no del tot fàcil, ja que el nexe d'unió ha de permetre conservar la major eficiència possible.

En aquest projecte hem dissenyat la capa intermèdia usant ITO (i Ag quan l'hem necessitat per a fer mesures) sobre una ETL (Electron Transport Layer) formada principalment per una difusió de fòsfor i, posteriorment, hem estudiat dos dels paràmetres que més ens podien afectar a l'eficiència.

Un dels paràmetres era la resistència sèrie, ja que ens interessa que la capa intermèdia sigui el menys resistiva possible per evitar pèrdues òhmiques. Per altra banda hem estudiat la passivació de la cel·la per estudiar la capacitat recombinant de la superfície de la cel·la.

Després dels experiments, hem observat que els nostres resultats son bons a temperatures relativament baixes (0 - 200 ° C), cosa que ens permet fabricar estructures en tàndem en aquestes condicions. No obstant això, per a temperatures elevades, els resultats no són prou bons i, tot i que es van realitzar experiments per intentar corregir la degradació amb la temperatura, no vam aconseguir un resultat adequat per a temperatures més altes.

Resumen

La humanidad ha tenido que confrontar diversidad de problemas durante su historia. Desde guerras y conflictos hasta pandemias y hambre. Hoy en día, uno de los problemas más grandes que tenemos como sociedad es el cambio climático que nos está arrastrando a un calentamiento global. Las alternativas a los combustibles fósiles están popularizándose, destacando por encima de todos la energía solar. En este documento trataremos una de sus limitaciones tecnológicas más grandes.

Las celdas solares tándem son una innovadora tecnología que nos permite unir dos o más celdas solares con diferentes propiedades de absorción del espectro de luz y así poder aumentar la eficiencia del sistema total. Unir las celdas es una tarea no del todo fácil, ya que la capa intermedia entre celdas debe permitir conservar la mayor eficiencia posible.

En este proyecto hemos diseñado la capa intermedia usando ITO (y Ag cuando lo hemos necesitado para hacer medidas) sobre una ETL (Electron Transport Layer) formada principalmente por una difusión de fósforo. Posteriormente, hemos estudiado dos de los parámetros que más nos podían afectar a la eficiencia.

Uno de los parámetros era la resistencia serie, ya que nos interesa que la capa intermedia sea lo menos resistiva posible para evitar pérdidas óhmicas. Por otra parte, hemos estudiado la pasivación de la celda para estudiar la capacidad recombinante de la superficie con el objetivo de obtener un sistema funcional.

Tras los experimentos realizados observamos que nuestros resultados son buenos a temperaturas relativamente bajas (0 – 200 °C), permitiéndonos fabricar estructuras tándem en esas condiciones. Sin embargo, para altas temperaturas los resultados no son lo suficientemente buenos y aunque se realizaron experimentos para intentar corregir la degradación con la temperatura, no conseguimos un resultado adecuado para temperaturas más elevadas.

A mi yaya Pilar, gracias por cuidar de mí todos estos años

Acknowledgements

I want to express my deepest gratitude to both of my research supervisors: Pablo Ortega, PhD and Gerard Masmitjà, PhD for guiding and providing me the opportunity to do a research on this project and for their unconditional help during the most critical procedures.

Next, I need to acknowledge Gema Lopez and all clean room users and technicians who helped me when I had issues on the usage of the instrumentation.

I also want to thank my family and specially my father for their unconditional support during the most difficult years of this journey which conclude with this project.

Finally, I want to express my gratitude to Alex, Juan Carlos and Pol, my friends and mates who made me saw this experience with other eyes when I was thinking to drop out.

Revision history and approval record

Revision	Date	Purpose
0	30/09/2020	Document creation
1	24/11/2020	First document revision
2	12/12/2020	Second document revision
3	12/01/2021	Third document revision

DOCUMENT DISTRIBUTION LIST

Name	e-mail
Albert Poblador Bonet	albert.poblador@estudiantat.upc.edu
Pablo Rafael Ortega Villasclaras	pablo.rafael.ortega@upc.edu
Gerard Masmitjà Rusiñol	gerard.masmitja@upc.edu

Written by:		Reviewed and approved by:	
Date	30/09/2020	Date	26/01/2021
Name	Albert Poblador Bonet	Name	Pablo Ortega Gerard Masmitjà
Position	Project Author	Position	Project Supervisor

Table of contents

Abstract ... 2
Resum ... 3
Resumen ... 4
Acknowledgements ... 6
Revision history and approval record ... 7
Table of contents ... 8
List of Figures ... 10
List of Tables: ... 12
1. Project plan ... 13
1.1. Introduction ... 13
1.2. Requirements and Specifications ... 14
1.3. Methods and procedures ... 14
1.4. Work plan ... 15
1.4.1. Work Breakdown Structure ... 15
1.4.2. Work Packages ... 15
1.4.3. Gantt Diagram ... 17
1.5. Deviations from the original plan and incidences ... 17
2. State of the art ... 18
2.1. Tandem Solar Cells ... 18
2.2. Interconnection Layer ... 19
3. Methodology: ... 20
3.1. Preparation and Deposition Techniques ... 20
3.1.1. Chemical attack with Hydrofluoric acid ... 20
3.1.2. RCA Cleaning ... 20
3.1.3. Sputtering ... 21
3.1.4. Thermal evaporation ... 22
3.2. Characterization Techniques ... 23
3.2.1. Four-Point Measurement ... 23
3.2.2. Transmission Line Measurements ... 24
3.2.3. Carrier Lifetime Measurements ... 26

3.2.4. Atomic Layer deposition 28

4. Results 29

4.1. Block 1: Main experiment 29

4.1.1. Specific contact resistance measurements with ITO/Ag on phosphorous diffusion regions 30

4.1.2. Passivation study 34

4.2. Block 2: Additional experiments 36

4.2.1. ITO Annealing before Ag deposit 36

4.2.2. Buffer layer using Atomic Layer Deposition 38

5. Budget 41

6. Environment Impact 42

7. Conclusions and future development: 43

Bibliography: 44

Appendix 1: List of all experiments performed 46

Appendix 2: Additional experiments 48

A. Deposit over glass 48

B. Deposit over non-doped wafer 49

C. Deposit over a wafer with an oxide layer 50

D. Creation of a buffer between ITO and Ag (no diffusion) 52

Glossary 53

List of Figures

Figure 1: Efficiency of different kind of solar cells[3] 13

Figure 2: Work Breakdown Structure 15

Figure 3: Series connected tandem solar cell[6] 18

Figure 4: Description of the absorption and thermalization losses occurring in a solar cell[7] 18

Figure 5: Efficiency of top and bottom solar cell vs band gap energy[6] 19

Figure 6: Leybold Systems UNIVEX 350 Sputtering machine from UPC clean room. 21

Figure 7: Sputtering process. [13] 21

Figure 8: Thermal evaporator [14] 22

Figure 9:Four-point probe technique[16] 23

Figure 10: Shadow mask used in the deposition of the contact layer to be able to be able to perform TLM measures [18] 24

Figure 11: A piece of the shadow mask with the parameters used for measurements indicated . 25

Figure 12: Parameters obtained from TLM measurements[19] 25

Figure 13: SINTON wafer Life-time tester used to obtain the passivation measurements 26

Figure 14: Example of an ALD complete cycle [22] 28

Figure 15: Structure of the TLM samples. 29

Figure 16: Structure of the TLM samples with specific resistances. 29

Figure 17: Structure of the passivation samples. 29

Figure 18: TLM measurement (as deposited) of ITO/Ag on three phosphorous diffusion temperatures. Measured with a contact distance of 0.25 mm. 30

Figure 19: TLM plot obtained for the sample with a R_{sh} of 50 Ω/Sq. The result shown in the plot is the average of measurement. The finger resistance contribution is subtracted. 31

Figure 20: I-V characteristic for the three samples after annealings. From left to right R_{sh} of: 25 Ω/Sq, 50 Ω/Sq and 100 Ω/Sq. Results are extracted from the measurements performed at a contact deistance of 0.25 mm. 32

Figure 21: Specific contact resistance for different sheet resistance values in linear scale. 33

Figure 22: Specific contact resistance for different sheet resistance values in logarithmic scale. . 33

Figure 23: Measured lifetime vs. Minority Carrier Density for several samples measured as deposited. 34

Figure 24: Effect of sheet resistance on the recombination current density of SiO_2 passivated (solid symbols) and ITO coated (empty symbols), phosphorous-diffused samples. Its effect with the annealing temperature is also shown. 35

Figure 25: Structure of the TLM sample for this experiment. 36

Figure 26: I-V characteristic for full ITO deposited experiments. The left image corresponds to the sample with a R_{sh} of 100 Ω/Sq and the right one corresponds to the sample with 25 Ω/Sq.......... 36

Figure 27: TLM measurement (as deposited) obtained without diffusion and with the buffer created of 6/20 ALD cycles.. 38

Figure 28: TLM measurement (as deposited) obtained with both phosphorous-diffusion (R_{sh} of 100 Ω/Sq) and a buffer of 6/20 ALD cycles. Measured with a contact distance of 0.25 mm. Its effect with the annealing temperature is also shown.. 39

Figure 29: TLM measurement (as deposited) with phosphorous diffusion (R_{sh} of 100 Ω/Sq), a buffer of 6/20 ALD cycles and an ultra-thin magnesium film. 39

Figure 30: TLM measurement obtained with phosphorous diffusion (R_{sh} of 100 Ω/Sq), a buffer of 6/20 ALD cycles and an ultra-thin magnesium film. Measurements as deposited and with the annealing treatments. The comparison is done with a TLM distance of 0.15 mm........................ 40

Figure 31: Evolution of the energy consumption in the UPC for the last twelve years [26]........... 42

Figure 32: I-V characteristic of the deposit over glass. The left image corresponds with the sample without annealing (As deposited) and the right one with an annealing at 300 degrees................ 48

Figure 33: I-V characteristic for ITO and Ag deposited over non-doped wafer (left) measured in 0.15 mm finger in comparisson with the slightly doped (R_{sh} = 100 Ω/Sq) sample used in 4.1.1 (right). 49

Figure 34: I-V characteristic for the sample with thermal oxide as deposited 50

Figure 35: I-V characteristic for the sample with chemical oxide 51

Figure 36: I-V characteristic for the samples with 6/40 (right) and 6/80 (left) as deposited 52

List of Tables:

Each table in the thesis must be listed in the "List of Tables" and each must be given a page number for its easy location.

Table 1: TLM parameters obtained for the sample with an R_{sh} of 50 Ω/Sq. 31

Table 2: TLM parameters for ITO/Ag over glass and phosphorous-diffused c-Si sample (R_{sh} = 100 Ω/Sq). 37

Table 3: Itemization of the products and handwork required for the development of this project. 41

Table 4: List of experiments performed in chronological order. 46

Table 5: Complete list of all wafers used and the samples that were used for experiments. In blue, the samples that were not used. 47

1. Project plan

1.1. Introduction

The most reasonable solution to avoid global warming is to change the way we produce and use the energy. Fossil fuels constitute our first source of energy, yet their pollution and future scarcity make them unsustainable. Thus, different ways of producing energy are becoming more popular, with the use of the sun as a source of green energy being the most promising.

Nowadays, solar panels can process up to 24.4% of solar light into usable energy [1] depending on different factors, such as placement, orientation, weather conditions… Solar cells are tested in different extreme conditions to ensure his reliability and his endurance during the pass of the years.

Countries with good climate conditions such as Spain can take profit of this and produce energy enough to not depend on fossil fuels. Thanks to this it can be possible to fulfil the requirements asked in Paris agreements such as keeping a global temperature rise this century well below 2 degrees Celsius above pre-industrial levels and to pursue efforts to limit the temperature increase even further to 1.5 degrees Celsius [2].

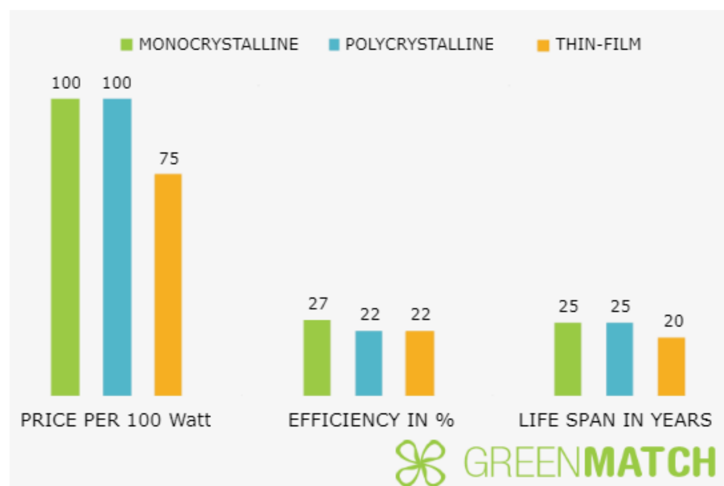

Figure 1: Efficiency of different kind of solar cells[3]

The use of solar energy in a domestic environment is not relatively high, however, the increase in the consumption of electrical energy (e.g. electric cars) and the use of it in more demanding environments, such as industries, poses a challenge for the photovoltaic industry. The motivation of this project relies in the fact that modifying fabrication conditions and testing new materials, a faster and easier transition to solar energy can be achieved.

1.2. Requirements and Specifications

The main objective of this project is to study the properties of indium-tin oxide (ITO) films deposited on phosphorous diffused (n^+) regions for its use as electron-selective contact on crystalline silicon (c-Si) solar cells. In addition, it must be compatible as a contact layer between the top and bottom absorbers in a tandem solar cell configuration. In this way, the studies focus on certain critical parameters that allow us to know if this layer is good enough to extract the electrons of the n-type c-Si absorber (i.e. ohmic contact and good passivation), and to connect both cells without degradation (i.e. support thermal processes).

The first stage is to create the contact layer. We decided to use ITO as it is commonly used as transparent conductive oxide (TCO), which means it is light transparent, allowing light to flow from the top cell to the bottom cell. ITO layers will be synthetized in the sputtering machine where we can deposit ITO on our c-Si wafer uniformly and control the thickness by modifying time exposure. On the one hand, we are going to study the contact resistance using transfer length method (TLM) [4]. On the other, we are going to study the contact passivation using lifetime measurements by Sinton instrument [5].

Finally, we will analyze the influence of temperature in the contact resistance and passivation by applying annealings at different temperatures. Concurrently, we will study the passivation and the effect of the recombination in our layer to know its long-term degradation with time including also the influence of temperature by processing annealings.

Project requirements:

- Learning of Clean Room working, oriented to the deposit of layers by Sputtering process, including cleaning methods of wafers and laboratory material.

Project specifications:

- Study of passivation to obtain effective recombination velocities (S_{ef}) lower than 100 cm/s, or recombination current densities (J_0) below 300 fA/cm^2.
- Achieve an ohmic contact resistance with specific contact resistance (ρ_c) lower than 100 mΩcm2 using n-type wafers.

1.3. Methods and procedures

This project is the continuation of Arnau Torrens bachelor thesis where he studied the Optimization of electron selective contacts for silicon solar cells. In his study, the results obtained using Titanium nitride (TiN_x) as an electron selective contact to possibly substitute magnesium/aluminum (Mg/Al) were not satisfactory enough. Nevertheless, at the end of the project, he experimented with new material, ITO on a phosphorous doped substrate (n^+) obtaining positive results opening the door to this project.

In addition, this project contains references to papers with previous studies developed by other laboratories with the idea in mind to emulate the results and compare the discrepancies obtained and so comment and investigate the because of the differences.

1.4. Work plan

The methodology to organize the project is the same used at the rest of the degree. The project is splitted in a work breakdown structure with different work packages. A Gantt diagram is elaborated taking in account that changes on time plan may depend on circumstances such as machines maintenance, broken samples or other inconveniences that we cannot control.

1.4.1. Work Breakdown Structure

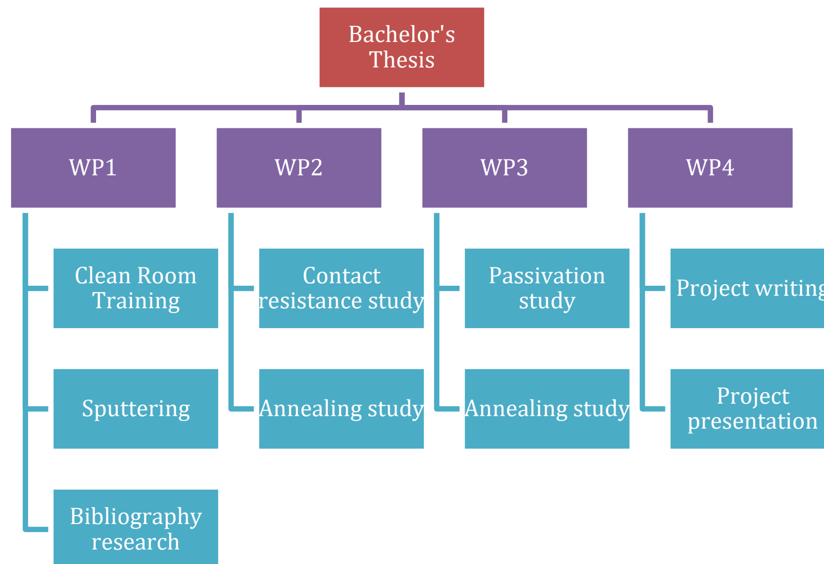

Figure 2: Work Breakdown Structure

1.4.2. Work Packages

<table>
<tr><td>Project:</td><td colspan="2">WP ref: WP1</td></tr>
<tr><td>Major constituent: Project Initiation</td><td colspan="2">Sheet 1 of 4</td></tr>
<tr><td rowspan="2">Short description:
(1) Learning clean room processes.
(2) Start looking for bibliography and previous studies.
(3) Start preparing the experimental samples.</td><td colspan="2">Planned start date:
Planned end date:</td></tr>
<tr><td colspan="2">Start event: 20/07/2020
End event: 23/09/2020</td></tr>
<tr><td>Internal task T1.1: Do Clean room training.
Internal task T1.2: Prepare the samples for the experiments.
Internal task T1.3: Bibliography search, start writing State-of-art.</td><td>Deliverables:</td><td>Dates:</td></tr>
</table>

Project:	WP ref: WP2	
Major constituent: Contact resistance study	Sheet 2 of 4	
Short description: (1) Learn Transmission Line Measurement basics and how to do the measurements. (2) Measure the contact resistance of the samples. (3) Perform annealing's at different temperatures and repeat the measurements. (4) Analyze the data obtained and study the variation of the contact resistance for each annealing temperature.	Planned start date: 27/07/2020 Planned end date: 30/11/2020 Start event: End event:	
Internal task T2.1: Transmission Line Measurements background. Internal task T2.2: Study as deposited. Internal task T2.3: Annealing study.	Deliverables: D1: Report of contact resistance study.	Dates:

Project:	WP ref: WP3	
Major constituent: Passivation study	Sheet 3 of 4	
Short description: (1) Influence of thickness in passivation. (2) If a good passivation is achieved study time degradation and accumulative annealings. (3) With the best cases (thickness and temperature annealing) test different annealing accumulative times.	Planned start date: 17/09/2020 Planned end date: 30/11/2020 Start event: End event:	
Internal task T3.1: Life-time measurements background Internal task T3.2: Study the passivation as deposited. Internal task T3.3: Annealing study.	Deliverables: D2: Report of passivation study.	Dates:

Project:	WP ref: WP4	
Major constituent: Project writing	Sheet 4 of 4	
Short description: (1) Writing of the bachelor's thesis. (2) Defense of the degree thesis.	Planned start date: 30/11/2020 Planned end date: 26/01/2021	
	Start event: End event:	
Internal task T4.1: Write thesis. Internal task T4.2: Presentation and thesis defense.	Deliverables: D3: Thesis	Dates:

1.4.3. **Gantt Diagram**

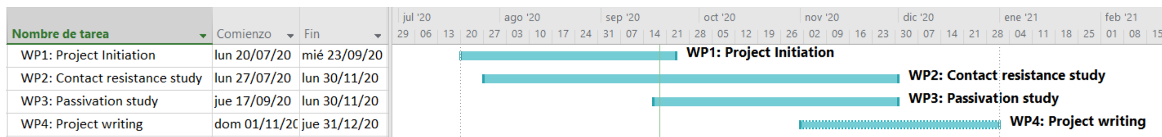

Nombre de tarea	Comienzo	Fin
WP1: Project Initiation	lun 20/07/20	mié 23/09/20
WP2: Contact resistance study	lun 27/07/20	lun 30/11/20
WP3: Passivation study	jue 17/09/20	lun 30/11/20
WP4: Project writing	dom 01/11/2(	jue 31/12/20

1.5. Deviations from the original plan and incidences

The project started in the middle of July 2020. This year has been specially complicated because of the SARS Covid-19 pandemic. The mobility limitations, prevention measures and other things derivate from the same, made us to adapt our schedule to the government indications. Nevertheless, we knew this problematic since the beginning so adapting the work plan was not a big problem.

Afterwards, the project was meant to be performed while I was realizing my internship in Everis. However, the incorporation to my job was delayed for 2 weeks and that gave me extra time to make progresses in my project and in this way, shorten the delivery times of the deliverables.

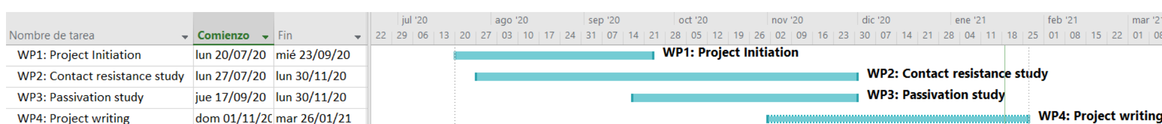

Nombre de tarea	Comienzo	Fin
WP1: Project Initiation	lun 20/07/20	mié 23/09/20
WP2: Contact resistance study	lun 27/07/20	lun 30/11/20
WP3: Passivation study	jue 17/09/20	lun 30/11/20
WP4: Project writing	dom 01/11/2(	mar 26/01/21

2. State of the art

To improve the efficiency of solar panels, researchers can take many different paths based on other technologies, on the modification of manufacturing materials... Nowadays, a lot of different studies can be found looking for the same objective.

2.1. Tandem Solar Cells

A good method to increase the efficiency of a solar cell is by splitting the light spectrum. Light, as electromagnetic wave has a frequential spectrum.

Tandem cells consist in individual or series connected cells which every cell is optimised to each section of spectrum. Series cells are simpler to fabricate but the current is the same through each cell so this constrains the band gaps that can be used.

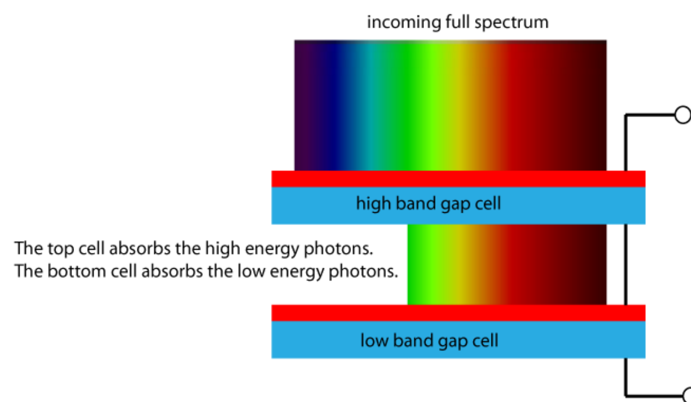

Figure 3: Series connected tandem solar cell[6]

The most common way to arrange these cells is to grow them monolithically so the cells are grown as layers and tunnel junctions connect the individual cells.

In the article written by *Ameri et al.* [7] are explained the most common losses of energy in solar cells, which are the absorption and thermalization losses. Only photons having an energy larger than the band gap of the photoactive materials can be absorbed and contribute to the photovoltaic conversion. Hot charge carriers created upon photon absorption relax down to the conduction band of the photoactive materials, giving rise to the so-called “thermalization”.

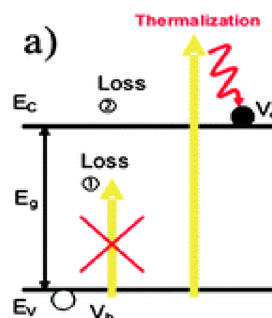

Figure 4: Description of the absorption and thermalization losses occurring in a solar cell[7]

These losses limit the efficiency of actual solar cells. A good idea to solve them is using tandem solar cells which performance has been studied by *De Vos* [8]. This author demonstrated that stacking several sub-cells in series allows theoretical efficiencies ways beyond the limitations, mostly due to an enhancement of the electrochemical potential of charge carrier extraction.

While the maximum efficiency under laboratory conditions of a single cell under non-concentrated sunlight is calculated to be around 30%, this value is raised to 42% for a tandem comprising two sub-cells, and to 49% for a tandem comprising 3 sub-cells.

As we can see, the results obtained by tandem cells are farer better than single junction cells (see Fig. 5) where depending on the materials used for the cells and the number of bandgaps, we can obtain higher efficiencies.

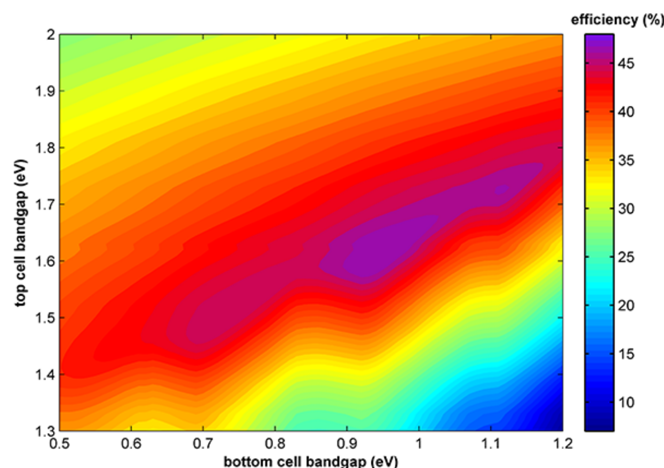

Figure 5: Efficiency of top and bottom solar cell vs band gap energy[6]

2.2. Interconnection Layer

It is important to say that losses between cells can be also an important threat to efficiency. For that reason, it is also important to design an intermediate layer which allows the transference of electrical energy between cells.

The most important characteristic that interconnection layer must have is the transparency because the bottom cell also needs to get light energy. Nowadays, studies with transparent materials have been performed to obtain higher transmittances. In the case of Al/MoO_3 an efficient charge collection to realize electric connection in series. For polymer-small molecule tandem cell, due to the summation 1.01 V of the open-circuit voltages of individual cells and a short-circuit current density of 6.05 mA/cm^2, a power conversion efficiency PCE of 2.82% was obtained under 100 mW/cm^2 illumination, which is larger than either of the individual cells [9].

Other promising material is Indium Tin Oxide (ITO) because it is properties of highly transparent over the visible spectrum (>80%), very low resistivity (~10^{-4} Ωcm), high carrier concentration (~1021 cm^{-3}) with mobility around 10–30 cm^2/Vs, wide optical band gap (~3.6–3.9 eV) and high work functions (~4.20 eV)[10]. So, the material chosen to create the interconnection layer is important to the future performance of the tandem solar cell.

3. Methodology:

3.1. Preparation and Deposition Techniques

3.1.1. Chemical attack with Hydrofluoric acid

The surface of silicon wafers easily reacts with oxygen, which is present in the ambient, creating silicon oxide (SiO_2), being a dielectric layer. In some experiments we were interested in removing this oxide layer and therefore the wafer is submerged in a hydrofluoric acid (HF) aqueous solution. The time and the concentration of HF may depend on the thickness of the SiO_2 film to be removed. In our application, the samples were dipped between 30 sec to 1 min in aqueous solution with a concentration of 1 - 2% of HF.

3.1.2. RCA Cleaning

RCA Cleaning is a technique that consists of a set of steps to perform a deep cleaning. It is commonly used to clean silicon wafers prior to perform high temperature processes. This technique was developed by Werner Kern at RCA Laboratories [11] in 1993. The chemical process is performed in the following sequence:

I. Removal of the organic contaminants, RCA1 (organic clean + particle clean).
II. Removal of thin oxide layer, HF1(oxide strip, optional).
III. Removal of ionic contamination, RCA2 (ionic clean).
IV. Removal of thin oxide layer, HF2 (oxide strip, optional).

Below is shown the recipe followed in our RCA cleanse process:

- RCA1: 1500 ml H_2O deionized (18 MΩ) + 250 ml H_2O_2 + 250 ml NH_3
- RCA2: 1500 ml H_2O deionized (18 MΩ) + 250 ml H_2O_2 + 250 ml HCl
- HF1&2: 99 ml H_2O deionized (18 MΩ) + 1 ml HF

Firstly, we introduced the wafers into the solution RCA1. Then we heated the solution at level 9 for 13 minutes and then 7 minutes more at level 3. (Levels of heat goes from 1 to 10 being the number 10 the hottest one). Then, the solution is quenched for 5 minutes under running water. Finally, a cleanse using HF at 1% of concentration for 1 minute. We repeat the sequence por the RCA2 bath.

3.1.3. Sputtering

Sputtering is a phenomenon in which microscopic particles of a solid material are ejected from its surface, after the material is itself bombarded by energetic particles of a plasma. Sputtering has different applications such as cleanses, analysis, etching… In our case we used this technique to deposit films of ITO in our silicon wafer. Fig.6 shows the Sputtering equipment used in the project.

Figure 6: Leybold Systems UNIVEX 350 Sputtering machine from UPC clean room.

Sputtering involves ejecting material from a target (e.g. ITO or Ag) onto a substrate (e.g. c-Si wafer or glass). As shown in Fig.7, this technique involves creating a gaseous plasma which is generated and confined to a space containing the material to be deposited. The surface of the target is eroded by high-energy ions within the plasma. Thus, the free atoms of the extracted material travel through the vacuum environment where some of them are deposited onto substrate creating a thin film.

In a typical process, the chamber is set to vacuum in order to minimize the potential contaminants. Once the desired pressured is reached, the sputtering gas is released, and then, the total pressure is regulated using a pressure controller. Plasma is generated using a high voltage between the cathode (located behind the target) and the anode (electrical ground). The electrons collide with the nearby atoms of sputtering gas causing ionization. In order to facilitate as many high energy collisions as possible – leading to increased deposition rates – the sputtering gas is typically chosen to be a high molecular weight gas such as argon or xenon [12].

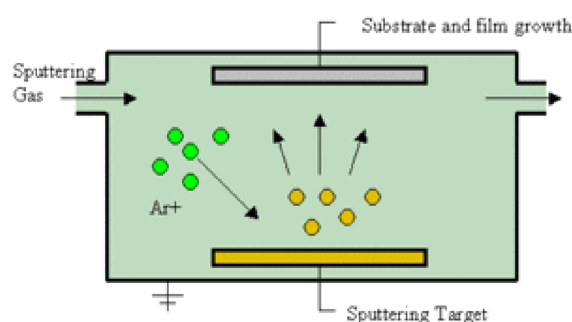

Figure 7: Sputtering process. [13]

The Sputtering process can deposit a uniform layer of material, as well as precisely control its thickness by exposure time. To create a pattern on the surface, we can use a shadow mask. In this way, the material will only be deposited on the surface through windows of the metal mask, which is placed on the substrate. For example, for TLM measurements we deposited the ITO/Ag contacts by shadow masks technique.

Nevertheless, a drawback of the Sputtering process is that passivation may decrease because of ions impact, which is commonly recovered by an annealing temperature step [5].

3.1.4. **Thermal evaporation**

Evaporation is another technique for film deposition. The material to be deposited is evaporated under vacuum conditions, which allows the material to travel from the source to substrate without reacting with the ambient particles. Like sputtering, it is important to set the chamber in vacuum to precisely control the layer thickness. Poor vacuum tends to create non continuous films.

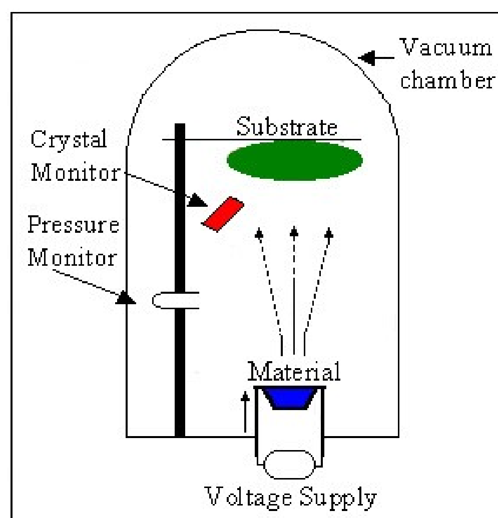

Figure 8: Thermal evaporator [14]

As shown in Fig.8, the material is deposited in ceramic boats. When enough temperature is reached, the material changes its state from solid to liquid or gas depending on the material characteristics (for example, manganese tends to sublimate). Once the material is in gas form, the particles travel to substrate which is placed above the source of material.

3.2. Characterization Techniques

3.2.1. Four-Point Measurement

The four-point measurement is a technique used to measure the Sheet resistance of thin films in semiconductors [15]. The mechanism includes four probes in which the current passes through exterior probes and the inner ones measure the voltage (see figure below).

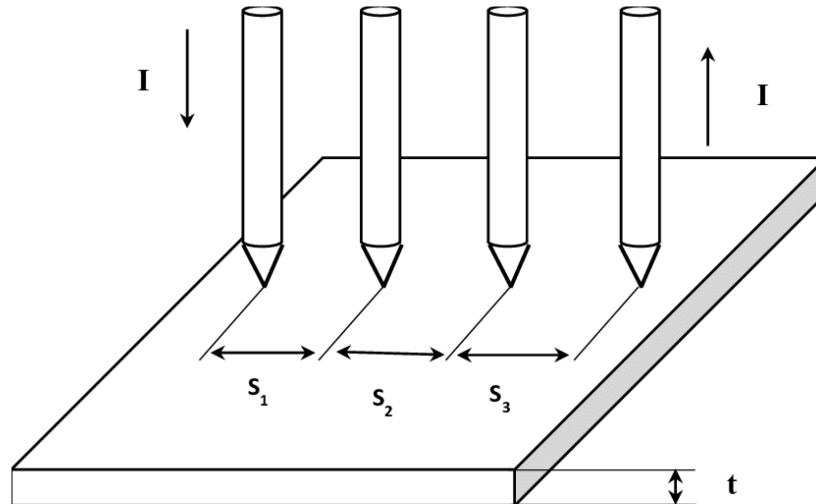

Figure 9:Four-point probe technique[16]

The potential difference between the two inner probes for equally separated points is obtained through the following equation [17] where *r1* and *r2* are the distances between the probes, *I* is the current and R_{sh} is the sheet resistance:

$$V = \frac{IR_{sh}}{\pi} \cdot \ln\frac{r1}{r2} = \frac{IR_{sh}}{\pi} \cdot \ln 2 \quad (1)$$

Rewriting the equation for obtaining the sheet resistance (R_{sh}) we obtain a slight variation of Ohm's law:

$$R_{sh} = \frac{\pi}{\ln 2}\frac{V}{I} = 4.53\ \frac{V}{I} \quad (2)$$

Once obtained the resistance, the resistivity is directly calculated from by multiplying for the thickness (*W*) of the wafer:

$$\rho_{sh} = R_{sh} \cdot W \quad (3)$$

3.2.2. Transmission Line Measurements

Transmission Line Method (TLM) or Transfer Length Method is a technique used to determine the contact resistance between a metal and a substrate. It consists in make a different series of contacts separated by different distances.

To create the samples, we deposited our contact (ITO/Ag) using the sputtering technique with the help of a shadow mask to form a TLM structure. Fig.10 shows an image of the shadow mask used, but in our case, we only work with a quarter of the mask because the experiments were performed using a quarter of c-Si wafer. Besides, with this mask the contact separation distances were 0.15, 0.25, 0.35, 0.45 and 0.55 mm theoretically.

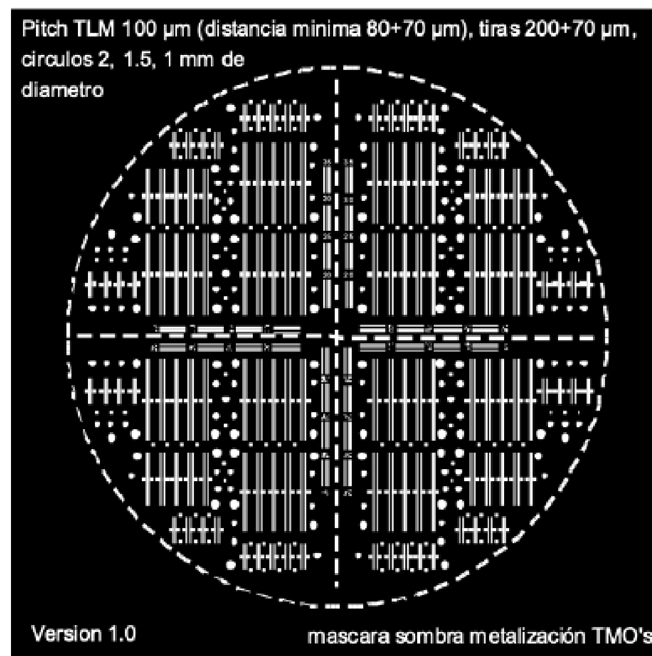

Figure 10: Shadow mask used in the deposition of the contact layer to be able to be able to perform TLM measures [18]

To perform the experiments, probes are applied to the pairs of contacts and the resistance between them is measured by applying a voltage across the contacts and measuring the resulting current.

The current flows from the first probe into the first metal contact. Then, it goes across the metal-semiconductor junction and through the sheet of semiconductor. Next, it flows across the metal-semiconductor junction again, although this time in the other direction, and into the second metal contact. From there, it goes into the second probe and into the external circuit to be measured. The resistance measured is a sum of the contact resistance of both metal contacts involved and the sheet resistance of the semiconductor in-between these contacts.

Once we have several results with different contact distances (d), a plot of resistance versus contact separation can be performed. The contact separation is expressed in terms of the ratio R_{sh}/W, where R_{sh} is the sheet resistance of the substrate and W is the width (see Fig.12). If the behavior of the measurements is ohmic, we should obtain a linear plot because of the Ohm's Law.

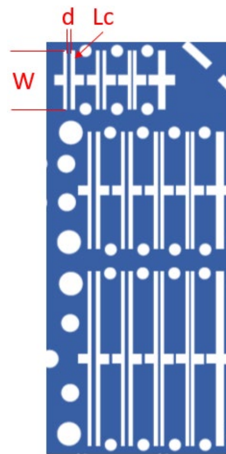

Figure 11: A piece of the shadow mask with the parameters used for measurements indicated

As it is explained before, with several measurements we can obtain a plot of resistance against contact distance (see Fig.12). According to D.K Schroder [4], it is possible to obtain specific parameters from the measurements obtained previously. We highlight the point where the line crosses the y-axis, which is two times the contact resistance (R_c).

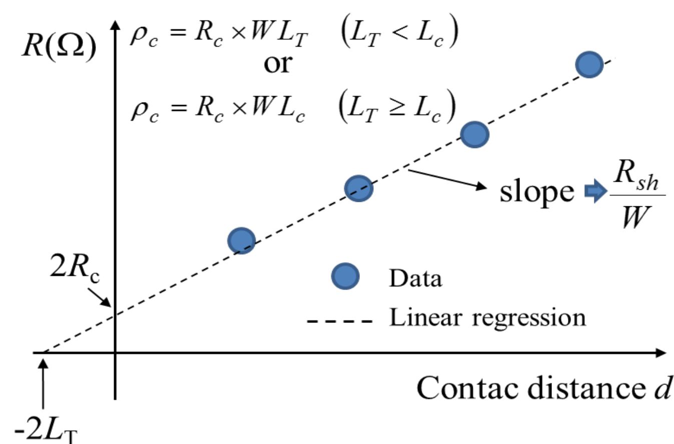

Figure 12: Parameters obtained from TLM measurements[19]

To obtain the specific contact resistance (ρ_c), we can use the following equation:

$$\rho_c = Rc \cdot W \cdot L_T \quad (L_T < L_C) \tag{4}$$

$$\rho_c = Rc \cdot W \cdot L_C \quad (L_T \geq L_C) \tag{5}$$

Where L_c is the length of the contact and L_T is the transfer length which is the effective length of the contact and it is obtained from the plot where is minus two times the point that crosses with the x-axis. The transfer length is an important parameter which allows us to know how efficient our contact is. If the transfer length is small, the contact is not very efficient. However, if the transfer length is large, means that the contact length is contributing to the measurements. That is the reason for having two different equations.

On the other hand, (4) and (5) are not mathematical expressions itself even than approximations. In [20] , Grover S. defines the L_T with the following mathematical expression:

$$L_T = \sqrt{\frac{\rho_C}{R_{SH}}} \tag{6}$$

With a mathematical analysis performed by the investigator which, is reported in the literature, it is obtained the complete expression for the ρ_c:

$$\rho_C = \left(\frac{R_C W}{coth\left(\frac{L_C}{L_T}\right)} \right)^2 \cdot \frac{1}{R_{SH}} \tag{7}$$

3.2.3. **Carrier Lifetime Measurements**

The carrier lifetime is the most important property of semiconductor materials for solar cells. The concept of carrier lifetime in semiconductors is like average life expectancy in humans. When light irradiates the semiconductor (i.e. absorber), thousands of electron-hole pairs are generated. Depending on the properties of the semiconductor material, the average time in which this pairs recombine (in humans it will be death) changes. Thus, a high value of lifetime means more possibility to reach their respective contact and contribute to the generation of electricity.

There are different ways to measure the lifetime depending on the way the excess of carriers is created in the semiconductor. The simplest and most common of them is to measure the conductance of the wafer and the way it changes with either illumination or time. This can be easily implemented by inserting the piece of silicon in a circuit that measures its resistance by forcing a flow of current through it and measuring the resulting voltage drop. More conveniently, the wafer can be placed over an inductor that forms part of a radio-frequency circuit, which also produces a voltage that is proportional to the conductivity of the wafer [5].

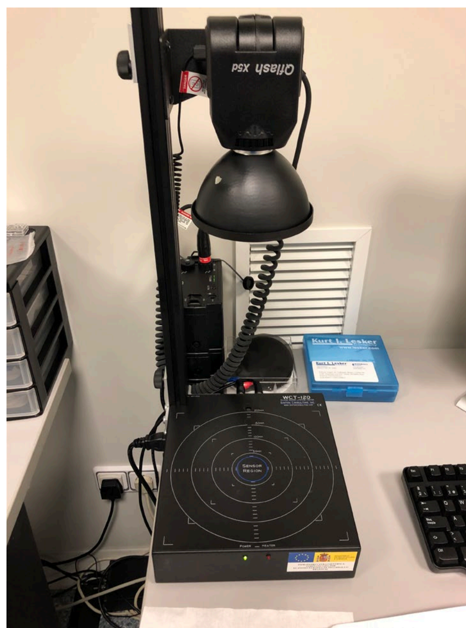

Figure 13: SINTON wafer Life-time tester used to obtain the passivation measurements

When light is shone on the wafer, the electron and hole concentrations increase in the same proportion producing as a result an increase on the photoconductance. The most important experimental parameter is the intensity of the illumination, which we can easily modify to produce different irradiance levels and consequently, modifies the electron-hole generation. The light intensity is measured thanks to a calibrated solar cell. Finally, with the photoconductance and the light intensity is it possible to obtain the effective carrier lifetime (τ_{eff}). Fig.13 shows the Sinton instrument used in the project to characterize the passivation property of the samples.

About the mathematics of the procedure, we can link the effective carrier lifetime, the τ_{bulk}, which is the bulk carrier lifetime and is intrinsically from the wafer and the width (W) with the recombination swiftness (S). Thanks to the work performed by Daniel Macdonald and Andrés Cuevas [5] we have a mathematical expression that helps us to obtain the interest parameters.

$$\frac{1}{\tau_{eff}} = \frac{1}{\tau_{bulk}} + \frac{2S}{W} \tag{8}$$

Moreover, the effective carrier lifetime can also be linked to the minority current density (J_0) which is the parameter that we worked with in this project. It is important to remark the fact that having a high current means that the recombination is increasing and therefore, the lifetime is decreasing.

However, the expression obtained in [5] has two different aspects depending on the injection of the carriers. It is important to realize that at very low injections the emitter may still influence the lifetime, while being indistinguishable from the bulk lifetime. This limitation on the measurable lifetime is particularly serious if the doping of the wafer is high and the emitter is itself not passivated, which usually results in a high J_0.

$$\frac{1}{\tau_{eff}} = \frac{1}{\tau_{bulk}} + \frac{2J_0}{qn_i^2 W} N_A \tag{9}$$

Of course, it is necessary to know apart from the previous explained parameters, the concentration of acceptor doping (N_A), the intrinsic concentration (n_i^2) and the charge of the electron which is a known constant.

On the other hand, when sufficiently high injection levels are achieved ($\Delta n \gg N_A$), the emitter contribution becomes much larger than the bulk recombination term and the effective lifetime essentially measures emitter recombination.

$$\frac{1}{\tau_{eff}} = \frac{2J_0}{qn_i^2 W} \Delta n \tag{10}$$

In addition, it is easy to create a relation between the effective recombination swiftness and the recombination current taking in account the low or high injection aspect.

$$S_{eff\ low\ injection} = \frac{J_0 N_A}{qn_i^2} \tag{11}$$

$$S_{eff\ high\ injection} = \frac{J_0 \Delta n}{qn_i^2} \tag{12}$$

3.2.4. **Atomic Layer deposition**

Atomic layer deposition (ALD) is a subclass of chemical vapor deposition technique that enables the deposition of an ultra-thin film of different types of oxides, with excellent uniformity [21]. The ALD process consists of sequential steps of pulses of gas precursors and purges, as it is shown in Fig.14.

During each reaction step, a precursor is pulsed into the chamber for a set pulse time to allow the precursor to react with the surface, obtaining a monolayer. Once it is deposited, the chamber is purged with an inner carrier gas such as N_2 in order to remove any remaining precursor that has not reacted.

Following the process, a second precursor is introduced in the chamber in a pulse as well and starts the second step of the surface reaction. After that, the chamber is purged again with an inert gas finishing in this way, a complete cycle, thus the more cycles, the thicker the layer will be. For example, to create alumina (Al_2O_3) we use trimethylaluminum ($Al_2(CH_3)_6$) and water (H_2O) which reacts inside the chamber and produces the desired component.

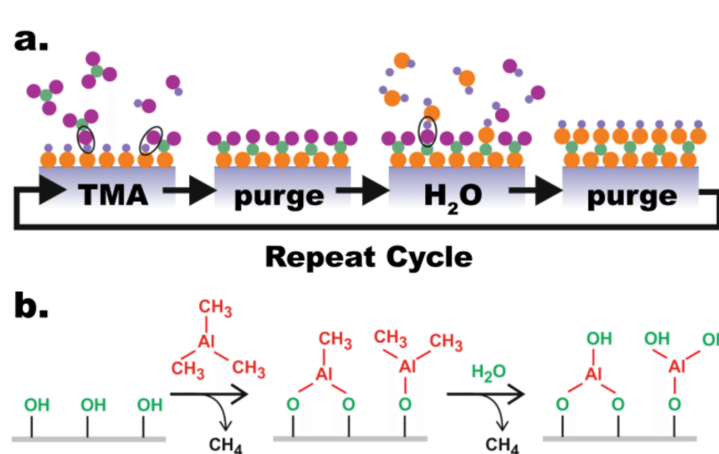

Figure 14: Example of an ALD complete cycle [22]

Nevertheless, it is important to mention that cycles can be created in our receipt using different proportions of the precursors. The proportions of the pulses do not have to be 1/1, it can be 1/2 or 1/4 depending on the specifications of the desired layer.

Advantages of ALD methods include uniform, conformal surface coverage with atomic scale thickness and composition control. Sequential precursor pulsing eliminates the potential for gas-phase reactions that result in film defects so that highly reactive precursors can be utilized.

Highly reactive precursors yield dense, continuous films with low levels of residual contamination and defects at relatively low process temperatures. High quality materials demonstrated include oxides, nitrides, metals, as well as complex multi-component films and multi-layered structures.

4. Results

This section of the dissertation presents the results obtained in the experimental section. For the analysis of the contact resistance we used the Transfer Length Method (TLM) and for the analysis of the passivation (i.e. recombination velocities or recombination current density) we used the lifetime measurements by Sinton instrument, as it is explained in the previous section.

4.1. Block 1: Main experiment

The main objective of this project which is explained several times in this report is to obtain a selective contact of electrons, optically transparent and resistant to temperature, using indium tin oxide (ITO) as a transparent conductive oxide and phosphorous diffusion (n^+) regions on c-Si (n) as electron transport layer (ETL).

Before starting with the results obtained, it is important to understand the structure of the complete system which is shown in the following figure:

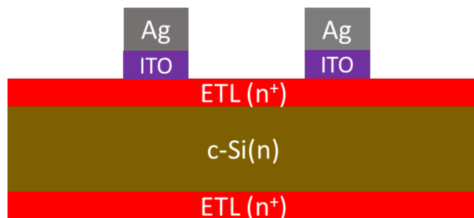

Figure 15: Structure of the TLM samples.

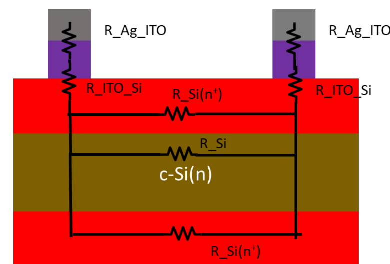

Figure 16: Structure of the TLM samples with specific resistances.

We can mount the equivalent system with the equivalent resistances that will be used to obtain the specific contact resistance with the TLM technique (see Fig.16). We are interested in finding a system with a resistance between ITO and silicon as low as possible. With the TLM measurements we can find the resistance of the complete set (see section 3.2.3).

About the passivation section, we are also interested in studying the passivation of the sample through the lifetime measurement of minority carriers. Since to obtain a good electron-selective contact two requirements must be met:

- An ohmic contact, in n-type wafer, with a very low specific contact resistance.
- A passivated contact (high lifetime), that is, a very low recombination current density.

We first study the passivation properties of thermally grown silicon oxide (SiO_2) on phosphorous diffused (n^+) samples. Then, we removed the SiO_2 from one side and we deposited the ITO film to observe the passivation properties of the n^+ region coated with ITO film. The structure is such that:

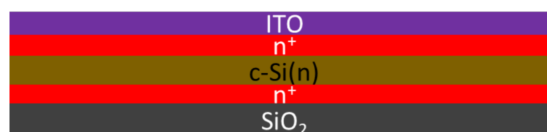

Figure 17: Structure of the passivation samples.

The study (TLM and passivation) was carried out with samples from three different phosphorous diffusion temperatures, which are subjected to the following process:

- RCA cleaning process
- Phosphorous diffusion through an oven at 835, 860 and 880 °C, using a phosphorous wafer as a dopant source.
- RCA Cleaning process
- Growth of a silicon oxide (SiO_2) layer, through an oven at 1000 °C rich in oxygen.

4.1.1. **Specific contact resistance measurements with ITO/Ag on phosphorous diffusion regions**

The specific contact resistance measurements were performed under some premises:

- We used wafers with different phosphor diffusions to study how diffusion strength affects the result.
- We study the effect of temperature (i.e. annealing) in TLM samples. It would be ideal if the temperature does not degrade the contact properties, since to build a tandem solar cell, such as c-Si/Kesterite, we need to subject it to temperatures above 400 °C.

Firstly, the samples were prepared using the techniques explained previously in this report (see Fig.15). Three different samples were used with diffusion temperatures of 835, 860 and 880 °C, resulting in sheet resistance (R_{sh}) of 100, 50 and 25 Ω/Sq, respectively. The temperature of diffusion is directly proportional to the R_{sh} of the diffusion. When higher is the temperature, lower is the R_{sh} and vice versa. Figure 18 shows the current-voltage (*I-V*) measurements of the three samples obtained with a TLM contact distance of 0.25 mm. It is important that at least, without an annealing step (as deposited) the behaviour is properly (i.e. ohmic).

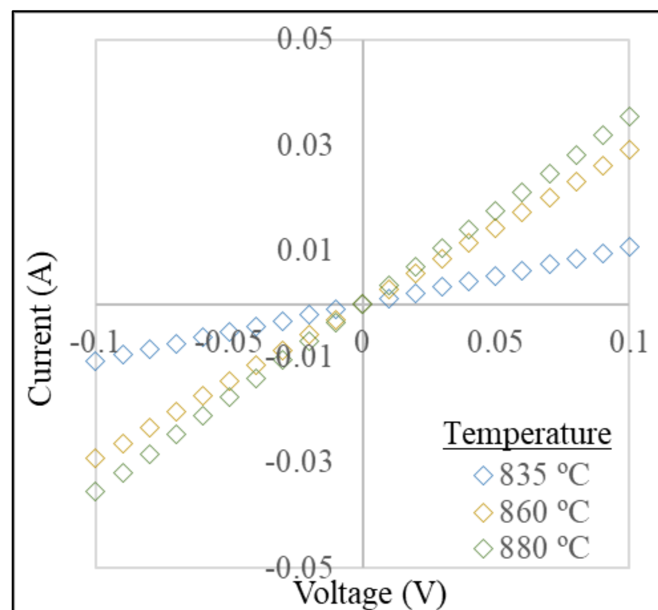

Figure 18: TLM measurement (as deposited) of ITO/Ag on three phosphorous diffusion temperatures. Measured with a contact distance of 0.25 mm.

In addition, it is observable that the *I-V* characteristic has a pronounced slope (see Fig.18) as diffusion gets stronger, which mean a lower contact resistance. In this way, we can observe that the characteristic is weakly ohmic when we have a soft diffusion (i.e. R_{sh} = 100 Ω/Sq) as it is expected.

So, apparently, is a good idea to have a strong diffusion (i.e. R_{sh} below 50 Ω/Sq) to ensure an ohmic behaviour of our sample. The main idea of this study is to obtain the lowest contact resistance in order to ensure the minimum losses due to that.

As it is explained in section 3.2.2 using the TLM technique we can obtain different parameters, such as ρ_c and R_{sh}. In our case it is interesting to obtain the specific contact resistance due to that parameter affects directly to the ohmic losses in our system.

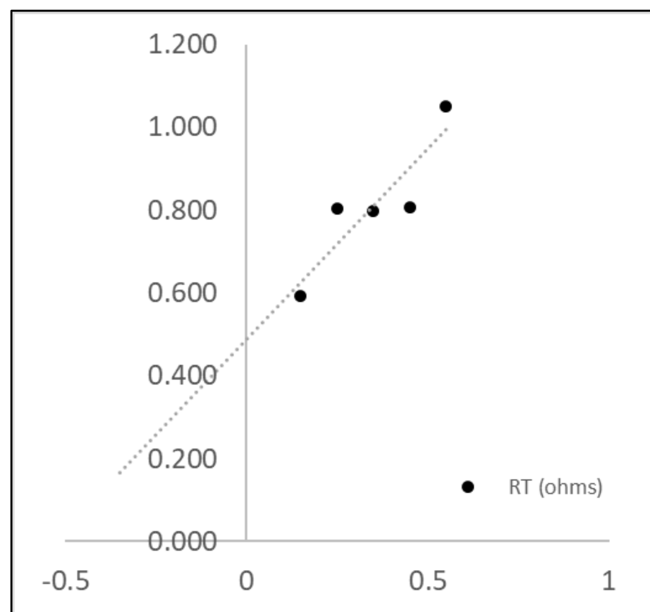

Figure 19: TLM plot obtained for the sample with a R_{sh} of 50 Ω/Sq. The result shown in the plot is the average of measurement. The finger resistance contribution is subtracted.

Comparing Fig.19 and Fig.12 we can appreciate some similarities between theoretical and experimental results which means that we are on the good track. As it is expected, it exists a biasing between the results obtained and the theoretical ones. In the following table we can see an example of the parameters obtained for one sample (i.e. 50 Ω/Sq).

Parameter	Average	Units
R_{sh}	13.8	Ω/Sq
R_c	0.244	Ω
L_T	0.201	mm
ρ_c	0.0056	mΩcm^2

Table 1: TLM parameters obtained for the sample with an R_{sh} of 50 Ω/Sq.

At first sight, the results obtained accomplish our needs for this project, obtaining values of ρ_c as low as 12, 18 and 98 mΩcm^2 for ITO contacting n$^+$ regions with R_{sh} values of 25, 50 and 100 Ω/Sq, respectively. Finally, it is important to study the behavior of the system with the temperature as we need also to subject it to temperatures above 400 °C.

The next step in our experiment was to expose our samples to different sets of temperature in an annealing process. These samples were exposed from 150 °C to 350 °C following steps of 50 °C for 10 minutes with forming gas (H_2N_2).

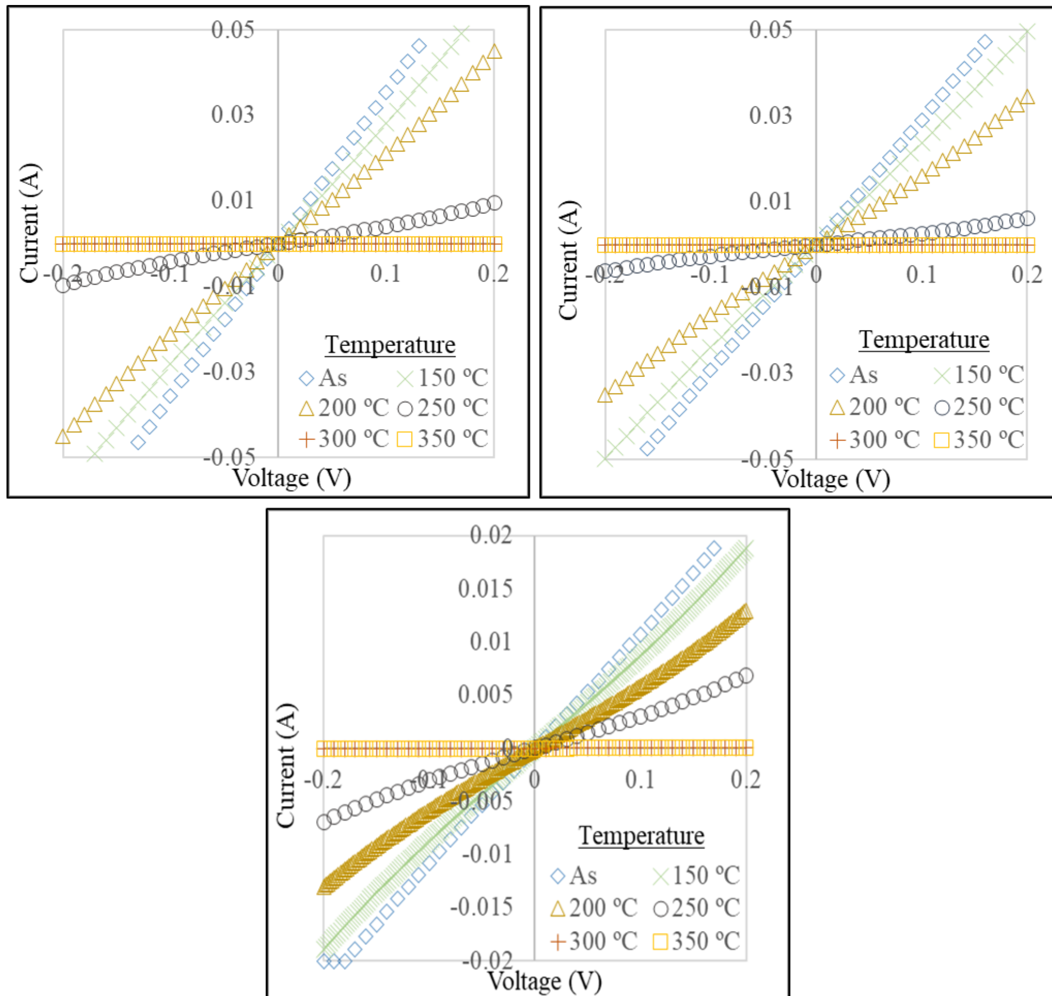

Figure 20: I-V characteristic for the three samples after annealings. From left to right R_{sh} of: 25 Ω/Sq, 50 Ω/Sq and 100 Ω/Sq. Results are extracted from the measurements performed at a contact deistance of 0.25 mm.

We observe that when the sample is exposed to temperature, the ohmic characteristic degrades, as the slope in the *I-V* curve is decreasing. We can conclude that n$^+$/ITO/Ag contact has an ohmic behaviour up to 200 °C. Nonetheless, above that temperature the characteristic is not ohmic compromising one of the objectives of the project which is to resist to higher temperatures.

Once we obtained the parameters for all the samples, we elaborated an analysis for extracting conclusions about our experiment. The following figures show the specific contact resistance (ρ_c) (measured in mΩcm^2) against sheet resistance of the phosphorous diffusion (measured in Ω/Sq).

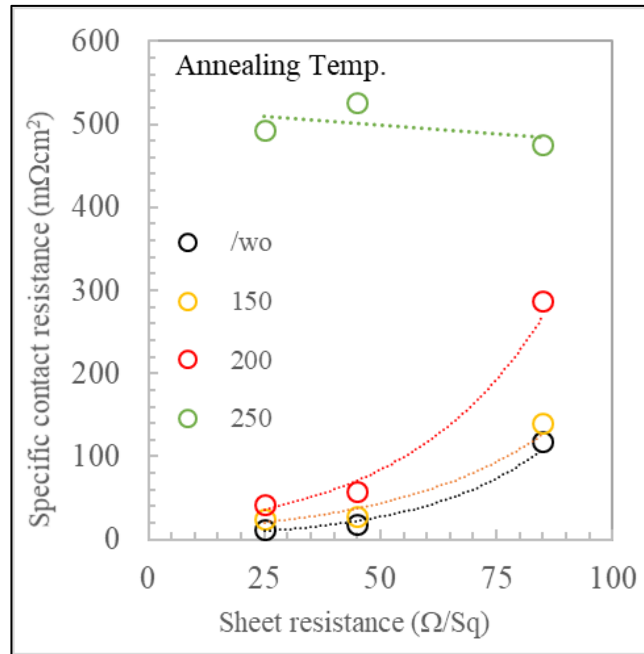

Figure 21: Specific contact resistance for different sheet resistance values in linear scale.

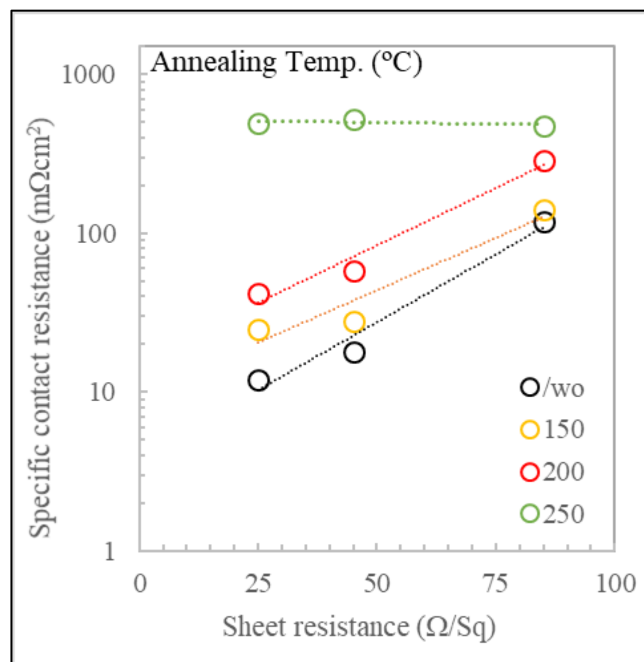

Figure 22: Specific contact resistance for different sheet resistance values in logarithmic scale.

We can observe two important things: First, the phosphorous diffusion plays an important role in the specific contact resistance and when the diffusion is strong, the resistance obtained is lower as it is expected. Secondly, the ρ_c quickly degrades with temperature above 200 °C.

Furthermore, it is important to mention that this specific contact resistance plotted in the previous graphics takes in account the contribution of the resistance between ITO and Ag. To study the contribution, we made an extra TLM study depositing ITO and Ag on a glass sample plate (see section 4.2 Block 2, table 2). Then we performed the *I-V* measurements obtaining the resistance of those materials. We obtained two different parameters with this study: Firstly, the sheet resistance

of the ITO layer with a value of 65 Ω/Sq, the value of which is like those obtained by other researchers [23]. Moreover, to contrast this value, we also applied the technique explained in section 3.2.1 to obtain the sheet resistance of the ITO layer. According to the four-point measurement the sheet resistance is 75 Ω/Sq which is quite like the value obtained with the TLM measurement.

The second interesting parameter is the specific contact resistance, which corresponds to the resistance between ITO and Ag films with a value of 6 mΩcm^2. It is important to take in account this result in order to obtain more precise results.

As a conclusion of these experiments we can say that our electron-selective contact formed by n^+/ITO/Ag stack works very well at low temperatures (below 100 °C), well at mid-range temperatures (below 250 °C) and even better if we use strong diffusions. Although, in a high temperature range we cannot use this selective contact scheme. That is why in following sections of this report (Block 2), we present our research to find a solution to overcome this problem.

4.1.2. **Passivation study**

It is necessary to have a very low recombination current density to obtain a high lifetime of the minority carriers and therefore to have a very good selective contact. Like the previous section, we used samples (see Fig.17) with different phosphorus diffusion temperature, and we studied how annealing process affects to the passivation properties.

One of the measurements we can obtain using the Sinton instrument is the lifetime of photo-generated carriers. This information is particularly interesting because we can visualize how well our measured lifetime is (i.e. passivation property) and compare it to the measurements performed by other researchers [24]. A first study was performed without annealing process (as deposited). In Fig.23 we can see the plot obtained with the measured lifetime *vs*. minority carrier density for three different phosphorus diffusion samples, the R_{sh} of which are 25, 50 and 100 Ω/Sq.

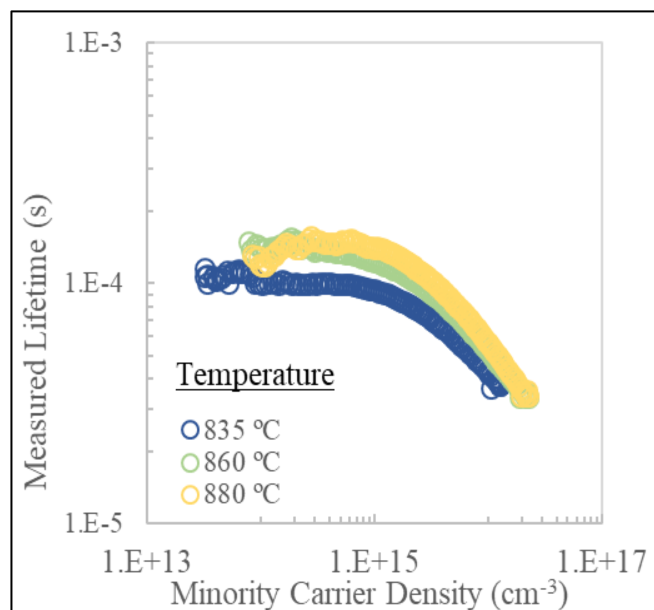

Figure 23: Measured lifetime vs. Minority Carrier Density for several samples measured as deposited.

The obtained measurements reveal interesting data. The sample with the strongest diffusion (lowest R_{sh}, 25 Ω) is the one with the highest lifetime, and the sample with the weakest diffusion (highest R_{sh}, 100 Ω) is the one with the lowest lifetime.

In addition, A figure of merit for passivation property is the effective recombination velocity (S_{eff}) or the recombination current density (J_0). A low value of those parameters is necessary to have a good selective contact. The Sinton instrument allows us to obtain the J_0 parameter, which permits us to study the influence of the annealing process at different phosphorus diffusion. Thus, in the next step we studied the effect of the annealing temperature in the passivation properties of n^+ samples coated with ITO film. The lifetime measurements can be seen in the annex section.

As a resume, in Fig.24 we can see the effect of the temperature in the recombination current density for different values of the sheet resistance from 25 to 100 Ω/Sq (the sheet resistance of the wafer is directly proportional to the strength of the phosphorus diffusion).

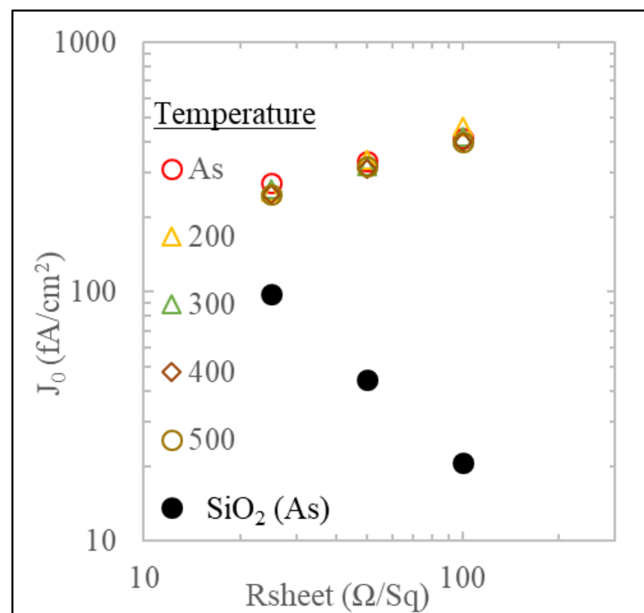

Figure 24: Effect of sheet resistance on the recombination current density of SiO_2 passivated (solid symbols) and ITO coated (empty symbols), phosphorous-diffused samples. Its effect with the annealing temperature is also shown.

When the n-type c-Si sample with phosphorus diffusion (n^+) on both sides is passivated by a SiO_2 layer we observe that the J_0 increases as the sheet resistance decreases. J_0 values as low as 21 fA/cm^2 have been measured for lightly doped samples, demonstrating a very good surface passivation. For samples with a strong diffusion (R_{sh} = 25 Ω/Sq) the J_0 parameter increase up to 100 fA/cm^2, denoting a poor passivation property. This phenomenon is well reported in the literature [25].

As expected, when the n^+ surface is covered with an ITO film (unpassivated surface) the contrary effect is shown. In this case, a strong phosphorus diffusion contributes to have a lower J_0 parameter, with a value of 273 and 412 fA/cm^2 for 25 Ω/Sq and 100 Ω/Sq, respectively. [25]

Finally, we can see that the effect of the temperature with the J_0 parameter is minimum. Thus, the passivation study concludes that our electron-selective scheme (n^+/ITO) has sufficiently good properties, from the passivation point of view, to be applied in solar cell devices.

4.2. Block 2: Additional experiments

In our main experiment we obtained an electron-selective contact that works properly with low temperatures. The main problem is that we may need to deposit materials to create the complete tandem cell with higher temperatures than 200 - 250 °C. With the information that we obtained previously is obvious that we need to do something more to ensure the stability at higher temperatures. In this section we show the investigations performed to solve this problematic.

4.2.1. ITO Annealing before Ag deposit

One hypothesis that we came up with is that Ag contact with ITO degrades with annealing, rather than c-Si/ITO interface. Therefore, we decided to deposit ITO over a n^+ c-Si wafer and then make a 300 °C annealing prior to Ag contact deposition. The idea was to anneal at a temperature that we knew that in the main experiment the results were not good enough and that is why we decided to make it at 300 °C. Then, we deposited the Ag with a shadow mask to make the contacts for TLM measurements (see Fig.25.)

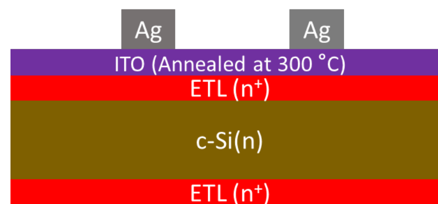

Figure 25: Structure of the TLM sample for this experiment.

Once the test samples were made with two phosphorous diffusion temperatures (i.e. R_{sh} values of 25 and 100 Ω/Sq) we measure the TLM structures. The *I-V* characteristic is plotted in Fig.26 showing an ohmic behavior.

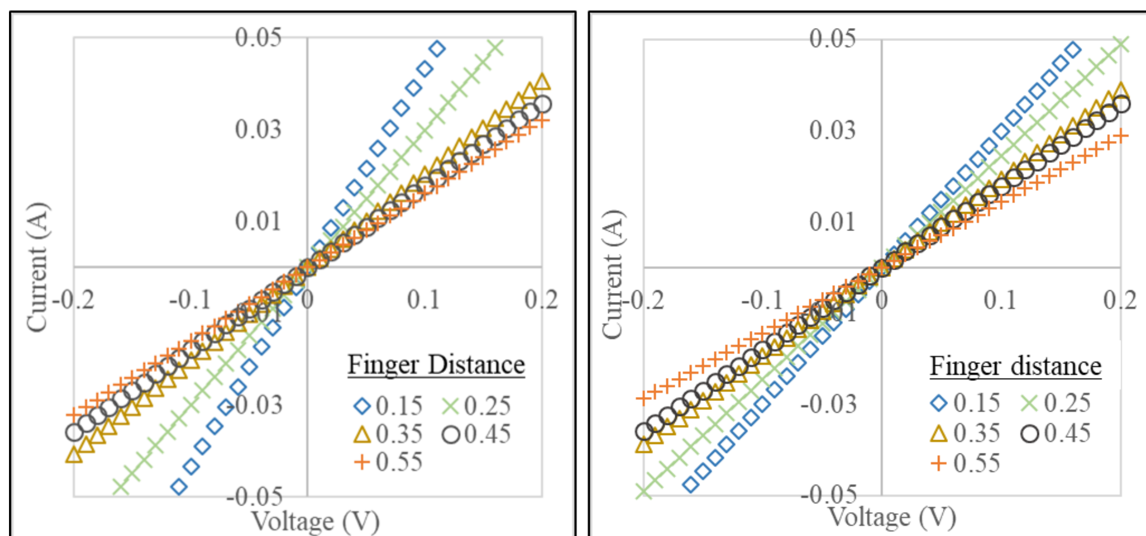

Figure 26: I-V characteristic for full ITO deposited experiments. The left image corresponds to the sample with a R_{sh} of 100 Ω/Sq and the right one corresponds to the sample with 25 Ω/Sq.

Nonetheless, ITO film is a conductive material and electrons tend to choose the less resistive way for moving. So, it was a possibility that electrons move through the ITO layer and no through the n^+ region like we wanted to. However, because we also did the experiment of depositing ITO and Silver over a glass plate, we could compare the results obtained with those and know if the electrons flow like we wanted to.

In the following table we can see the parameters measured with the weakest diffused c-Si sample compared to the glass ones:

	Glass (As)	Glass (300 °C)	c-Si (300 °C)
R_{sh} (Ω/Sq)	64.8	243.5	139.4
R_c (Ω)	0.421	0.1	0.1
L_T (mm)	0.095	0.047	0.041
ρ_c (mΩcm^2)	0.006	0.005	0.002

Table 2: TLM parameters for ITO/Ag over glass and phosphorous-diffused c-Si sample (R_{sh} = 100 Ω/Sq).

On one hand, the measured c-Si sample shows a high R_{sh} value than the phosphorous diffusion (i.e. 139 *vs*. 100 Ω/Sq). A possible reason for that is the fact that the electron conduction flows through the ITO instead of doing it for the ETL, which is not the behavior that we expect. Moreover, to ensure that conclusion we calculated the equivalent theoretical sheet resistance if the performance was like we wanted to:

$$R_{sh} = \frac{1}{\frac{1}{R_{ETL}}+\frac{1}{R_{c-Si}}+\frac{1}{R_{ETL}}} = \frac{1}{\frac{1}{100}+\frac{1}{50}+\frac{1}{100}} = 25\ \Omega/\mathrm{sq} \quad (11)$$

Therefore, the parallel value between 243 Ω/Sq (R_{sh} of ITO at 300 °C) and 25 Ω/Sq (theoretical R_{sh} of the sample) is what we should obtain with the TLM measurements. The higher value indicates that something happens between the different interconnected layers that makes our contact not good enough.

It is important to observe the results as deposited and after an annealing in the case of the ITO and Ag over the glass. In which we make sure not to break the hypothesis of the ITO and Ag contact does not degrade with temperature. Observing those values which are similar among them (6 and 5 mΩcm^2), we can say that the Ag/ITO contact works properly.

As a conclusion, we note that most of the electrons could flow through the ITO layer, pointing out that the contact between silicon and ITO is not good enough when a 300 °C anneal is performed.

4.2.2. **Buffer layer using Atomic Layer Deposition**

The previous experiment corroborates that the ITO/c-Si interface degrades with temperature, so one idea that we came up with is to put a buffer layer made from alumina (Al_2O_3) and titanium oxide (TiO_2). As it is explained in the methodology section, the main advantage of use the ALD technique is the quasi absolute control of the thickness of the layer. The idea is that this buffer also acts like an ETL and reinforces the actual one that we use in the main experiment (n^+). The Al_2O_3/TiO_2 stack is being used as ETL in c-Si solar cells within the research group, so it may be suitable as a buffer film for ITO/c-Si contacts. In this way, 6 and 20 ALD cycles of Alumina and TiO_2 were chosen, respectively, which means a final thickness of around 1.5 nm.

This section is made up of three different experiments. Firstly, we created the buffer over a wafer with no phosphor diffusion. The idea was to study if the behavior was whether ohmical or not without this n^+ layer. The premise under this idea is that if we can obtain a system that works well in this way, when we add a phosphor diffusion (stronger ETL) it will work better. The results obtained with TLM measurements can be seen in the following figure:

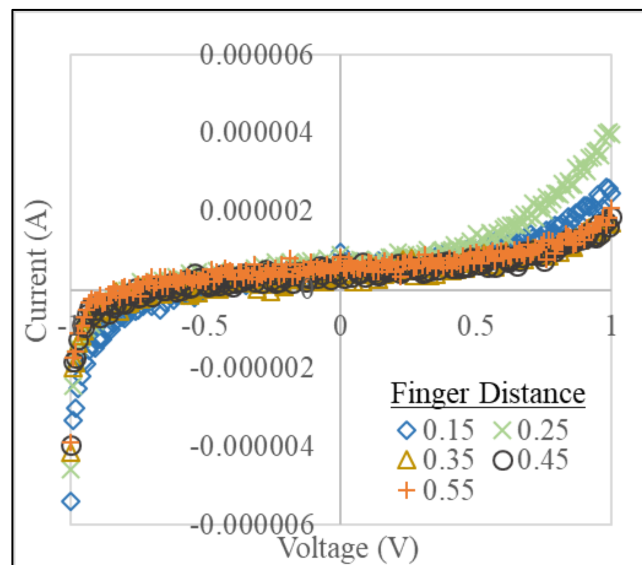

Figure 27: TLM measurement (as deposited) obtained without diffusion and with the buffer created of 6/20 ALD cycles.

As we can see, the *I-V* result obtained is far from being ohmic behavior and that leads us to the second part of the experiment. In this case we repeated the experiment but using a wafer with a phosphorous diffusion (R_{sh} of 100 Ω/Sq) expecting that the results would be better (see Fig.28). The main reason for using the weakest diffusion is because if we can ensure good results in that case, stronger diffusions therefore should be even better.

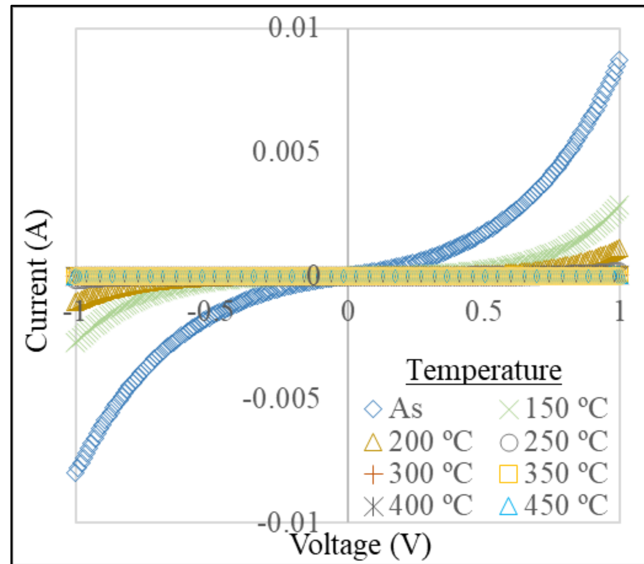

Figure 28: TLM measurement (as deposited) obtained with both phosphorous-diffusion (R_{sh} of 100 Ω/Sq) and a buffer of 6/20 ALD cycles. Measured with a contact distance of 0.25 mm. Its effect with the annealing temperature is also shown.

Even though the results are better with diffusion, are even far from being ohmical and that leads to the third and final part of our experiment. As the last attempt to force a better conduction and try to have an ohmic behavior is to deposit magnesium along with ITO and silver in the hope of improving results. It is important to say that a very thin layer is inserted, approx. 10 nm, to justify that it does not introduce many losses at an optical level, keep in mind that metals are not transparent, and we need transparent coatings.

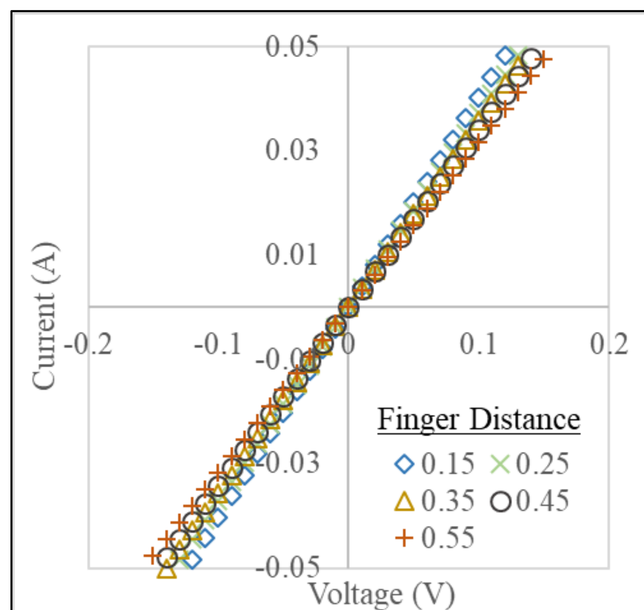

Figure 29: TLM measurement (as deposited) with phosphorous diffusion (R_{sh} of 100 Ω/Sq), a buffer of 6/20 ALD cycles and an ultra-thin magnesium film.

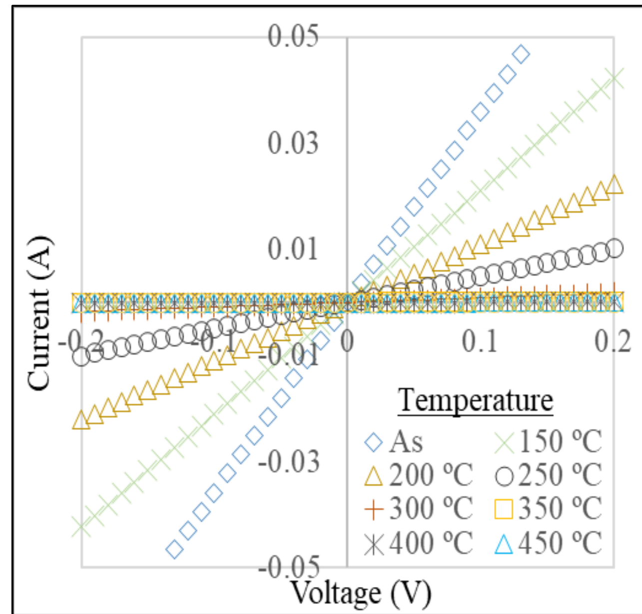

Figure 30: TLM measurement obtained with phosphorous diffusion (R_{sh} of 100 Ω/Sq), a buffer of 6/20 ALD cycles and an ultra-thin magnesium film. Measurements as deposited and with the annealing treatments. The comparison is done with a TLM distance of 0.15 mm.

With magnesium we improve conduction, obtaining a ρ_c value as low as 70 mΩcm^2, which means an improvement of 28 mΩcm^2 respect to the sample contacted directly with ITO film, for a same n$^+$ diffusion (100 Ω/Sq). As we can see in Fig.29, the *I-V* plot is purely ohmic and may be the solution for obtaining a good ohmical contact.

Nonetheless, with annealing temperature the contact degrades (see Fig.30) like the previous ones. This result is very promising, compared to the sample that does not have the 6/20/Mg since we observe in the results that the specific resistance has decreased, but more research is needed to find a solution with the annealing steps.

5. Budget

This project is part from an investigation performed by the Micro and Nanotechnology group of the Polytechnical University of Catalonia and is fully financed by the investigation group. In the following table are shown the prices of the materials used for the development of this project from zero.

Materials	Euros	Details	Quantity
Target ITO	500 €	2 inches	1
Target Ag	345 €	2 inches	1
Magnesium (Thermal evaporator)	34 €	10 g	1
Aluminium (Thermal evaporator)	41 €	50 g	1
N_2 Bottle	54.52 €		1
Ar Bottle	59.8 €		1
Forming Gas (H_2N_2) Bottle	62 €		1
Silicon wafers	40 €		7
TLM probes	1 €		2
HF (Fluorhydric Acid)	47 €	2,5 l	1
AlF (Aluminium fluoride)	66 €	2,5 l	1
NH3 (Ammonia)	39 €	2,5 l	1
Junior Electronic Engineer	9 €/h	450 h	
TOTAL PRICE			5580,32 €

Table 3: Itemization of the products and handwork required for the development of this project.

6. Environment Impact

One of the reasons that led me do this bachelor thesis was to investigate and give an impulse to the actual situation of the renewable energies. As it is explained at the introduction section, the actual efficiency of solar cells is not high enough for industrial uses, which lead those corporations to use fossil fuels instead of clean energy.

The obtained results, as a first laboratory prototype, do not have an environmental impact. Nevertheless, and looking with perspective, those open a door which may lead to an improvement of tandem cells efficiency.

The experiments were performed in Campus Nord installations, which is propriety of the Polytechnical University of Catalonia (UPC). UPC is very compromised about the use of renewable energies and every year makes a report called “Informe SIRENA” that is a resume of the energy and water wasted every year and the improvements made to be a more sustainable institution.

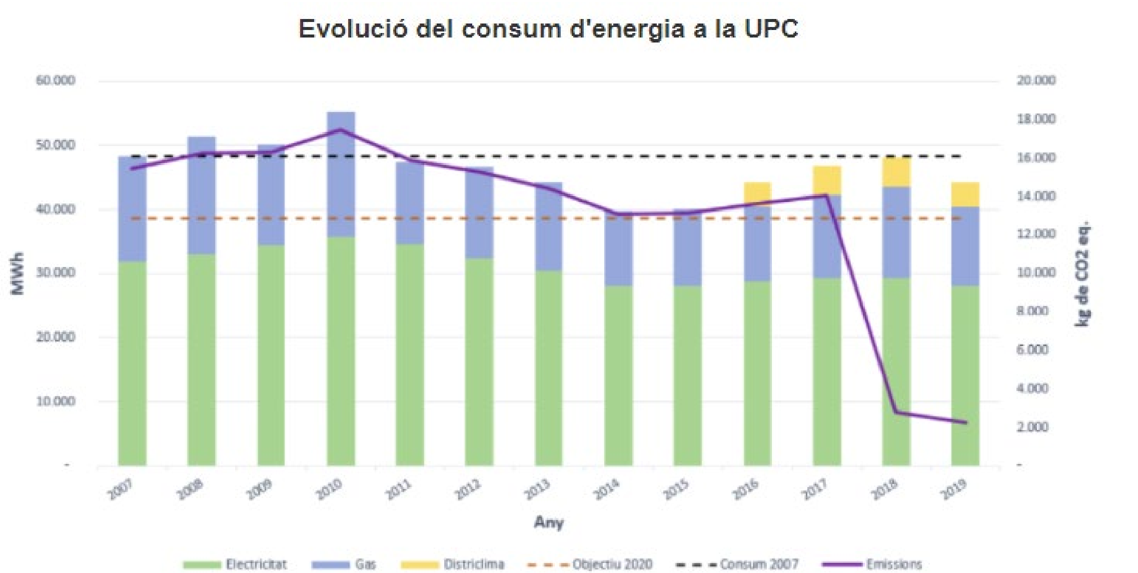

Figure 31: Evolution of the energy consumption in the UPC for the last twelve years [26]

At the beginning of each year, SIRENA is published at UPC network. In 2019, the construction of a 170 kW photovoltaic solar plant on the North Campus began and the project of 7 new facilities located on the North Campus, EPSEM, EPSEVG, FME, EPSEB and ESEIAAT, which will add 400 kW of power. Although, energy expenditure has been reduced by 9% thanks to the improvement of purchase prices and the reduction of consumption. This has represented a saving of approximately € 500,000 [26].

As a conclusion, the environmental impact of my project can be seen in two perspectives. Firstly, the results may contribute to make in a future, a cleaner way to produce and treat energy. On the other hand, the environmental cost of develop this project is low thanks to the improvements done by UPC to reduce the use of fossil fuels.

7. Conclusions and future development:

On this project we experimented using ITO over phosphorous diffusion samples to develop the interconnection layer for a tandem solar cell. With the objective to have J_0 values below 300 fA/cm^2 and ρ_c values lower than 100 mΩcm^2 as a minimum requirement.

After several experiments using phosphorous diffusion samples, we obtained promising results at lower temperatures making this technology ideal for create tandem cells at low temperatures. Lifetime and TLM measurements show J_0 values as low as 273 fA/cm^2 and ρ_c values of only 12 mΩcm^2, respectively. Nevertheless, when annealing temperature treatments were performed, we observed a high degradation of the contact resistance for temperatures above 250 °C.

On the other hand, with the passivation study revealed us that the effect of the temperature in the carrier lifetime is negligible. Moreover, recombination currents are lower in highly doped samples which tell us that is better to make stronger diffusions.

The first hypothesis behind the contact malfunction for temperatures above 250 °C is that the contact between ITO and Ag degrades with the temperature due to the crystallization of the ITO film. For clarify that theory, we performed an experiment consisting of depositing an ITO layer over the phosphorous doped sample (full covered), anneal with temperature and then deposit the Ag metal contact (TLM pattering). This experiment gave us promising results as the characteristic was strongly ohmic and the contact resistance inside our specifications. However, we did not know whereas the current flowed for the ITO layer instead of the wafer. So, we also deposited ITO and Ag over a laboratory glass substrate and measured the contact resistance to make a comparison with the c-Si substrate sample. The result shows that the current flows through the ITO layer instead of c-Si substrate. Therefore, there is a degradation between the c-Si/ITO interface, which prevents current flow towards the wafer, this being our second hypothesis.

With the idea to circumvent the c-Si/ITO interface degradation we investigated the effect of using a buffer film between the c-Si substrate and the ITO layer made from alumina (Al_2O_3) and titanium oxide (TiO_2) stack. However, the ohmic characteristic was not achieved on the first attempt (i.e. 6/20 ALD cycles of Al_2O_3/TiO_2). In order to resolve that problem, we added an ultra-thin magnesium film (~10 nm) to the buffer layer to improve the conduction, which led to very promising results. we measured a specific contact resistance as low as 70 mΩcm^2, which is smaller compared to the ρ_c obtained without the buffer layer. Nevertheless, it also degrades with temperature when the buffer plus magnesium is added.

As a conclusion, phosphorous diffusion region contacted with ITO film acts as an electron-selective contact, giving a good performance on tandem solar cells which require lower temperatures of fabrication. Nevertheless, whereas the temperature needed is higher, more than 200 °C, this structure cannot be used.

More research is needed to overcome contact degradation due to annealing temperature treatment. We point out two ways, using a thinner silicon oxide film (<2 nm), being able to be tunneled (i.e. n^+/SiO_2/ITO structure). Another alternative could be the use of ITO films deposited at temperature (during the sputtering deposition step). It is well known that ITO film crystallizes at temperatures above 150 °C, which could make it possible to obtain a much stable n^+/ITO contact structure at annealing process.

Bibliography:

[1] "Champion Photovoltaic Module Efficiency Chart | Photovoltaic Research | NREL." https://www.nrel.gov/pv/module-efficiency.html (accessed Nov. 18, 2020).

[2] "The Paris Agreement | UNFCCC." https://unfccc.int/process-and-meetings/the-paris-agreement/the-paris-agreement (accessed Nov. 18, 2020).

[3] "Which Solar Panels Are Most Efficient? −." https://solarlove.org/which-solar-panels-most-efficient/ (accessed Sep. 16, 2020).

[4] D. K. Schroder, *Semiconductor Material and Device Characterization*. Hoboken, NJ, USA: John Wiley & Sons, Inc., 2005.

[5] A. Cuevas and D. Macdonald, "Measuring and interpreting the lifetime of silicon wafers," *Solar Energy*, vol. 76, no. 1–3, pp. 255–262, Jan. 2004, doi: 10.1016/j.solener.2003.07.033.

[6] C. Honsberg and S. Bowden, "Tandem Cells | PVEducation." https://www.pveducation.org/pvcdrom/tandem-cells (accessed Sep. 18, 2020).

[7] T. Ameri, G. Dennler, C. Lungenschmied, and C. J. Brabec, "Organic tandem solar cells: A review," *Energy and Environmental Science*, vol. 2, no. 4. The Royal Society of Chemistry, pp. 347–363, Mar. 31, 2009, doi: 10.1039/b817952b.

[8] A. de Vos, "Detailed balance limit of the efficiency of tandem solar cells," *Journal of Physics D: Applied Physics*, vol. 13, no. 5, pp. 839–846, May 1980, doi: 10.1088/0022-3727/13/5/018.

[9] D. W. Zhao, X. W. Sun, C. Y. Jiang, A. K. K. Kyaw, G. Q. Lo, and D. L. Kwong, "Efficient tandem organic solar cells with an intermediate layer," *Appl. Phys. Lett*, vol. 93, p. 83305, 2008, doi: 10.1063/1.2976126.

[10] A. H. Ali, A. Shuhaimi, and Z. Hassan, "Structural, optical and electrical characterization of ITO, ITO/Ag and ITO/Ni transparent conductive electrodes," *Applied Surface Science*, vol. 288, pp. 599–603, Jan. 2014, doi: 10.1016/j.apsusc.2013.10.079.

[11] KERN and W., "Cleaning Solution Based on Hydrogen Peroxide for Use in Silicon Semiconductor Technology," *RCA Review*, vol. 31, pp. 187–205, 1970, Accessed: Oct. 10, 2020. [Online]. Available: https://ci.nii.ac.jp/naid/10022499434.

[12] "Magnetron Sputtering Overview." https://angstromengineering.com/tech/magnetron-sputtering/?utm_campaign=sputter_group&utm_medium=cpc&utm_source=sputter_group&gclid=Cj0KCQiA48j9BRC-ARIsAMQu3WRbvXrRQ3mcsb4DuqQK4jTRvkASXLIn2u1AI6ruguNvgQoYI_A_w84aAhK8EALw_wcB (accessed Nov. 24, 2020).

[13] "Sputter deposition - Wikipedia." https://en.wikipedia.org/wiki/Sputter_deposition#Gas_flow_sputtering (accessed Sep. 18, 2020).

[14] "Kurt J. Lesker Company | Frequently Asked Questions - Is there a method to calculate precisely how much material is needed to make a thin film of a given thickness by thermal evaporation? | Vacuum Science Is Our Business." https://www.lesker.com/newweb/faqs/question.cfm?id=487 (accessed Oct. 05, 2020).

[15] H. Chandra, S. Allen, S. Oberloier, N. Bihari, J. Gwamuri, and J. Pearce, "Open-Source Automated Mapping Four-Point Probe," *Materials*, vol. 10, no. 2, p. 110, Jan. 2017, doi: 10.3390/ma10020110.

[16] "Schematic demonstrating the setup of the four-point probe technique. | Download Scientific Diagram." https://www.researchgate.net/figure/Schematic-demonstrating-the-setup-of-the-four-point-probe-technique_fig15_275651666 (accessed Oct. 10, 2020).

[17] F. M. Smits, "Measurement of Sheet Resistivities with the Four-Point Probe," *Bell System Technical Journal*, vol. 37, no. 3, pp. 711–718, 1958, doi: 10.1002/j.1538-7305.1958.tb03883.x.

[18] A. Torrens, "Optimization of electron selective contacts for silicon solar cells," 2020.

[19] "TLM measurement | PVEducation." https://www.pveducation.org/pvcdrom/tlm-measurement (accessed Dec. 17, 2020).

[20] S. Grover, "Effect of Transmission Line Measurement (TLM) Geometry on Effect of Transmission Line Measurement (TLM) Geometry on Specific Contact Resistivity Determination Specific Contact Resistivity Determination," 2016. Accessed: Sep. 11, 2020. [Online]. Available: https://scholarworks.rit.edu/theses.

[21] "Kurt J. Lesker Company | Atomic Layer Deposition (ALD) – General, Technical, & Process Information | Vacuum Science Is Our Business." https://www.lesker.com/newweb/vacuum_systems/deposition_systems_ald_overview.cfm (accessed Dec. 12, 2020).

[22] "Schematic representation of Atomic Layer Deposition (ALD) of aluminum... | Download Scientific Diagram." https://www.researchgate.net/figure/Schematic-representation-of-Atomic-Layer-Deposition-ALD-of-aluminum-oxide-via_fig1_323178202 (accessed Oct. 18, 2020).

[23] M. J. Alam and D. C. Cameron, "Optical and electrical properties of transparent conductive ITO thin films deposited by sol-gel process," *Thin Solid Films*, vol. 377–378, pp. 455–459, Dec. 2000, doi: 10.1016/S0040-6090(00)01369-9.

[24] R. A. Sinton, "Quasi-Steady-State photoconductance, a new method for solar cell material and device characterization."

[25] M. J. Kerr, J. Schmidt, A. Cuevas, and J. H. Bultman, "Surface recombination velocity of phosphorus-diffused silicon solar cell emitters passivated with plasma enhanced chemical vapor deposited silicon nitride and thermal silicon oxide," *Journal of Applied Physics*, vol. 89, no. 7, pp. 3821–3826, Apr. 2001, doi: 10.1063/1.1350633.

[26] "Informe SIRENA 2019. Avaluació del consum d'energia i aigua de la UPC. — UPC Energia 2020 - Comunitats sostenibles — UPC. Universitat Politècnica de Catalunya." https://www.upc.edu/energia2020/ca/noticies/informe-sirena-2019-avaluacio-del-consum-d2019energia-i-aigua-de-la-upc (accessed Nov. 28, 2020).

[27] "Quantum tunnelling - Wikipedia." https://en.wikipedia.org/wiki/Quantum_tunnelling (accessed Dec. 28, 2020).

[28] D. L. Young, W. Nemeth, S. Grover, A. Norman, B. G. Lee, and P. Stradins, "Carrier-selective, passivated contacts for high efficiency silicon solar cells based on transparent conducting oxides," in *2014 IEEE 40th Photovoltaic Specialist Conference, PVSC 2014*, Oct. 2014, pp. 1-5A, doi: 10.1109/PVSC.2014.6925147.

Appendix 1: List of all experiments performed

In this section of our dissertation it is explained the complete list of the experiments performed for this report. Even though the result section contains the main experiments which can respond to our hypothesis, more experiments had to be performed to get the conclusions.

On the one hand, you will find the results which are also shown in the results section of the experiment and helped to respond our hypothesis. On the other hand, you will find the experiments which also were performed but due to the results obtained which did not helped at all to resolve our questions were discarded in first instance.

The objective of this section is none other than explain other ways of investigation that have been tried but which results were not satisfactory enough. Following to this explanation, you will find the complete list in the following table:

Experiment	Block	Date
Specific contact resistance measurement	1	September 2020
Passivation study	1	September 2020
Deposit over glass	2 /Appendix	October 2020
ITO Annealing before Ag deposit	2	October 2020
Deposit over non-doped wafer	Appendix	October 2020
Deposit over a wafer with oxide layer	Appendix	October 2020
Create a buffer between ITO and Ag (no diff)	2 /Appendix	October 2020
Create a buffer between ITO and ETL (n^+)	2	November 2020
Create a buffer (plus Mg) between ITO and ETL (n^+)	2	November 2020
Deposit the ITO film at temperature in Sputtering	FAILED	November 2020

Table 4: List of experiments performed in chronological order.

In Table 4, we can see the experiment done from September 2020 until November 2020. The experiments performed in July 2020 were discarded because some of them were done as a training and not for the purposes of this report.

The experimental part of this dissertation started on July 2020 with the clean room training and ended up in November 2020 due to Covid-19 restrictions. More information about this can be found on section 1.5.

In addition, to have an internal control of what experiments we have performed we created a table with each sample with its own code and the treatment that they had received:

Code	Diffusion (°C)	R_{sh} (Ω/sq)	Al_2O_3/TiO_2 (cycles)	SiO_2 (nm)	Mg (nm)	ITO (min)	Ag (min)	Annealing (°C)
Ti4A	835	85	6/20	-	-	60	15	150 - 350
Ti4B	835	85	6/20	-	-	60	15	150 - 350
Ti4C	835	85	6/20	-	-	60 full	-	-
Ti4D	835	85	-	-	-	60 full	-	-
Ti5A	835	85	-	-	-	60 full	15	300 before Ag
Ti5B	835	85	-	-	-	60 full	-	150 - 500
Ti5C	835	85	6/20	-	-	60	15	150 - 500
Ti5D	835	85	6/20	-	10	60	15	150 - 500
Ti7A	860	45	-	-	-	60	15	150 - 350
Ti7B	860	45	-	-	-	60 full	-	150 - 500
Ti7C	860	45	-	-	-	-	-	-
Ti7D	860	45	-	-	-	-	-	-
Ti6A	880	25	-	-	-	60	15	150 - 350
Ti6B	880	25	-	-	-	60 full	15	300 before Ag
Ti6C	880	25	-	-	-	60 full	-	150 - 500
Ti6D	880	25	-	-	-	-	-	-
Ti14A	-	-	-	2	-	60	15	150 - 500
Ti14B	-	-	-	2	-	-	-	-
Ti14C	-	-	-	2	-	-	-	-
Ti14D	-	-	-	2	-	-	-	-
Ti15A	-	-	6/20	-	-	60	15	150-500
Ti15B	-	-	6/40	-	-	60	15	150-500
Ti15C	-	-	6/80	-	-	60	15	150-500
Ti15D	-	-	-	-	-	-	-	-
Ti8A	-	-	6/20	-	-	30 temp	15	-
Ti8B	-	-	-	-	-	60	15	150-400
Ti8C	-	-	-	SiO_x	-	60	15	150-400
Ti8D	-	-	-	-	-	-	-	-

Table 5: Complete list of all wafers used and the samples that were used for experiments. In blue, the samples that were not used.

In Table 5 we can find the complete list of samples classified in function of the annealing temperature, diffusion, oxide layer, time of sputtering deposition and if they had or not an ALD buffer layer. This methodology allowed us to have a good control of what we were making in each moment of the experimental part and study what were the next step of the process.

Nevertheless, some samples were not used because of the specifications of experiments performed. In some cases, we needed samples which came from the same wafer in order to have the most similar initial conditions possible and that, made impossible to reuse some of them that were free. On the other hand, those samples can be used in experiments performed by the department which requires a single sample or other specifications that the investigator decides.

Appendix 2: Additional experiments

In this section of the dissertation can be find the experiments that were not critical to respond the hypothesis made at the start of the dissertation but were interesting enough to be added to the report. In Appendix 1 can be found the list of the experiments that will be shown in this section besides the ones mentioned in other sections of the report.

The objective of this appendix is to give a vision of what we performed as well as the results shown in the report and why we consider interesting enough to consider it.

A. Deposit over glass

The experiment consisted of depositing ITO and Ag over a laboratory sample plate with the purpose of compare the results obtained with the ones in 4.2.1. The conclusions extracted with this comparison can be found in the previous referred section. With the objective of demonstrate those results, this section will complement the information previously explained and give evidence.

ITO and Ag for TLM measurements were deposited in the same way as the other samples, only changing the deposit surface but respecting the sputtering times. In the following figures are shown the *I-V* characteristic obtained:

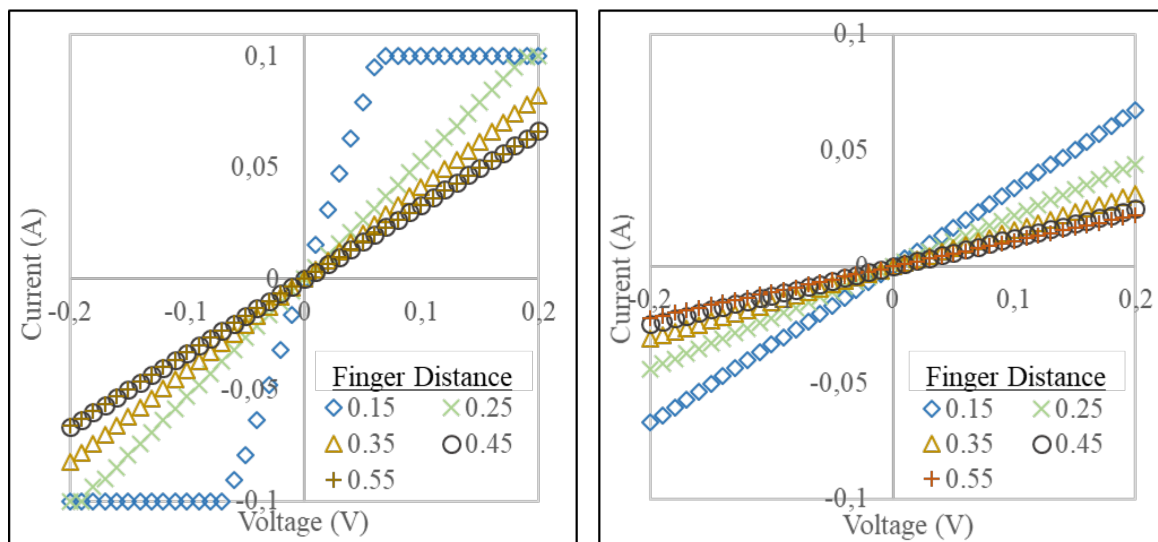

Figure 32: I-V characteristic of the deposit over glass. The left image corresponds with the sample without annealing (As deposited) and the right one with an annealing at 300 degrees.

The characteristic obtained in Fig.32 shows a good ohmical behavior (in both samples) despite of the degradation produced by the annealing. Even though, the results compared to ones in the literature shows a correspondence with the ones performed with other investigators. Afterwards, TLM technique were performed and the parameters obtained, and its interpretation can be seen in Table 2 and section 4.2.1.

B. Deposit over non-doped wafer

The main idea of this experiment was not to confirm the hypothesis more than to reaffirm the idea of the necessity of having a phosphorous diffusion. Even though the experiment may seem pointless it is useful and interesting to confirm that idea. In experimental work you must not discard any hypothesis without testing even if it seems pointless.

The experiment was performed in the same way as the experiment explained in 4.1.1 but changing the initial conditions of the wafer.

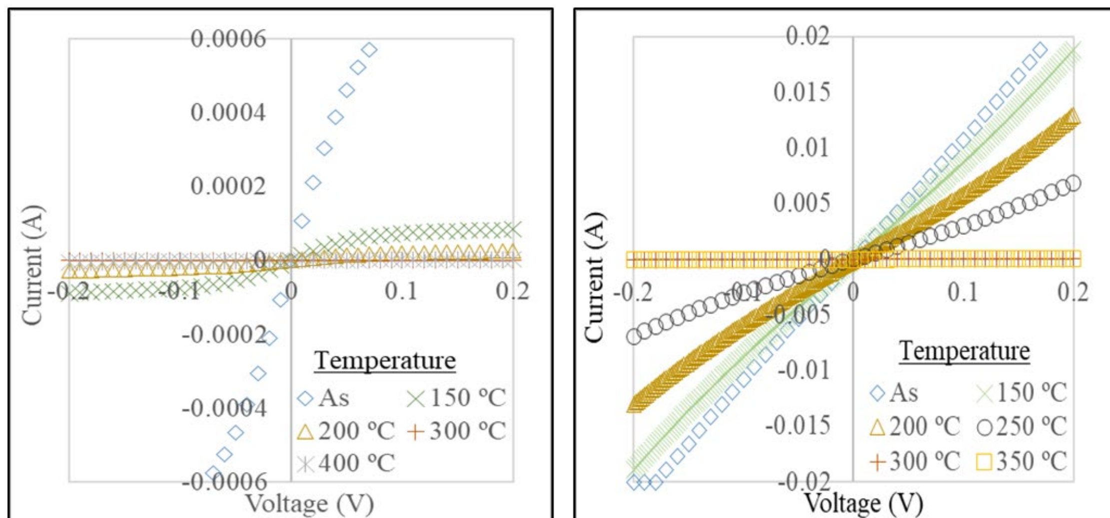

Figure 33: I-V characteristic for ITO and Ag deposited over non-doped wafer (left) measured in 0.15 mm finger in comparisson with the slightly doped (R_{sh} = 100 Ω/Sq) sample used in 4.1.1 (right).

Comparing both plots in Fig.33 two conclusions were extracted. Firstly, that the result obtained is far from following an ohmical characteristic which was expected from the beginning. Secondly observing the axis, the current flowing is small enough to consider that the conduction is quasi negligible when there is no diffusion.

Once obtained this result, the TLM technique was not performed due to the results obtained, which would not give us more information that we could consider useful. Considering the results, we confirmed the need of having a diffusion in our wafer.

In conclusion, we observe that it is necessary to have a diffusion to achieve an ohmic contact and completing the conclusion extracted in section 4.1.1, the stronger is the diffusion, the better are the results.

Nevertheless, since create a diffusion over a wafer is extra work, some experiments were performed over non-doped wafer because if the expected results were better, over a doped one they would have been better.

C. Deposit over a wafer with an oxide layer

In this section, we considered the idea of tunneling effect in our experiment and the benefits that may report, so a thermal silicon oxide (SiO_2) was grown with a specific furnace over a c-Si sample without phosphorous diffusion. Thickness of the SiO_2 layer was 2 nm, measured by ellipsometry equipment, being the limit of tunneling thickness.

In addition, this experiment consists of two different samples which on one of them we growth an oxide thanks to RCA technique (refer to section 3.1.2) with the purpose of observing if we observe tunnelling. Quantum tunnelling is the quantum mechanical phenomenon where a wavefunction can propagate through a potential barrier. The transmission through the barrier can be finite and depends exponentially on the barrier height and barrier width [27].

The idea of putting and oxide between the c-Si and ITO comes from the idea that indium, from the ITO layer, diffuse into c-Si substrate. Considering that indium is an acceptor impurity (p) it counteracts the phosphorous atoms, which are donor impurities (n), degrading the behavior of the electron-selective contact. Adding an oxide between ITO and c-Si may help to reduce the impurities diffused to the c-Si acting like a barrier.

Considering quantic physics, the potential level of silicon oxide is high enough to difficult the conduction and make our system not suitable to work. Even though, if the silicon layer is thin enough, tunneling may be produced and the conduction may be fulfilled. That is why it is important to have a thin layer.

In [28], investigators developed a study based in this technique with promising results using a thin silicon layer which we tried to reproduce in our laboratory installations. As it is explained before, we used two samples. Firstly, we have a thermal oxide (SiO_2) growth with a furnace which was expected to be uniform and without impurities.

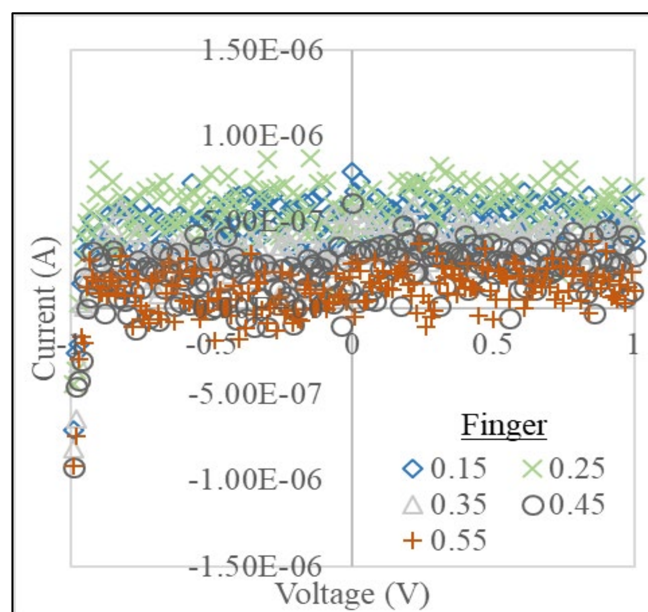

Figure 34: I-V characteristic for the sample with thermal oxide as deposited

Observing Fig.34, the results obtained are utterly bad. It is obvious that the behavior is not ohmic. The system does not conduct electricity (looking at the Y-axis), which is consistent with the dielectric nature of SiO_2 film, pointing out that the film thickness may be greater than 2 nm, thus the tunneling effect is not possible. Even though, the results shown in Fig.34 is as deposited, some annealings until 500 degrees were performed but no improvement was observed.

Secondly, we tried to do the same experiment with a chemical oxide (SiO_x) growth using RCA technique. This oxide was supposed to be not as uniform and pure like the one grown using the furnace but was interesting to compare different techniques for growing the oxide and decide which way works better.

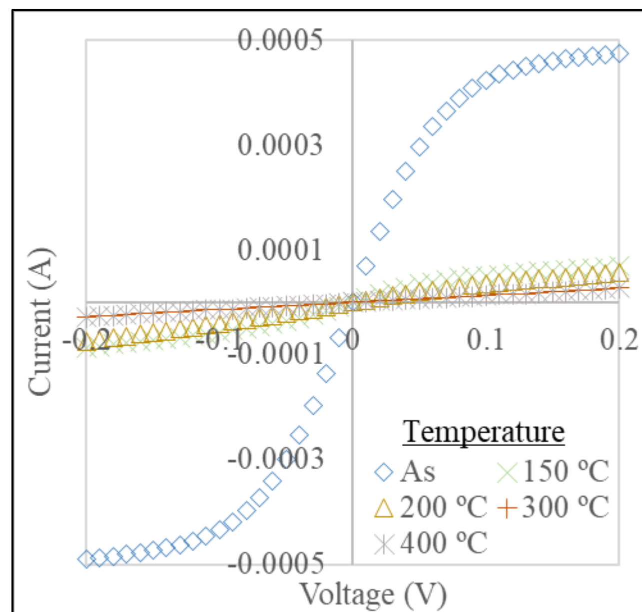

Figure 35: I-V characteristic for the sample with chemical oxide

In this case, the results were a bit better even though there is not conduction (that was expectable considering that both samples did not have a phosphorous diffusion). Once obtained the results as deposited, we studied the effects of the annealing process. In this case we show the results because we can note difference between temperatures not like the sample with the thermal oxide.

As a conclusion, the use of a tunneling SiO_2 and SiO_x film does not improve the contact specifications. Further research must be done by reducing the film thickness or by using phosphorous doped samples. This way should be explored in future project which start from this thesis.

D. Creation of a buffer between ITO and Ag (no diffusion)

This experiment is partly explained in section 4.2.2. Nevertheless, since some of the results were pointless for the hypothesis were not included in the results section despite some of them were interesting enough.

In section 4.2.2 it is shown a sample which received 6/20 ALD cycles of Al_2O_3/TiO_2. However, two more buffers were studied in order to find the effect of having buffers with different compositions. Two more samples were created using 6/40 and 6/80 ALD cycles of Al_2O_3/TiO_2. Afterwards, we analyzed qualitatively the effect by plotting the *I-V* characteristic.

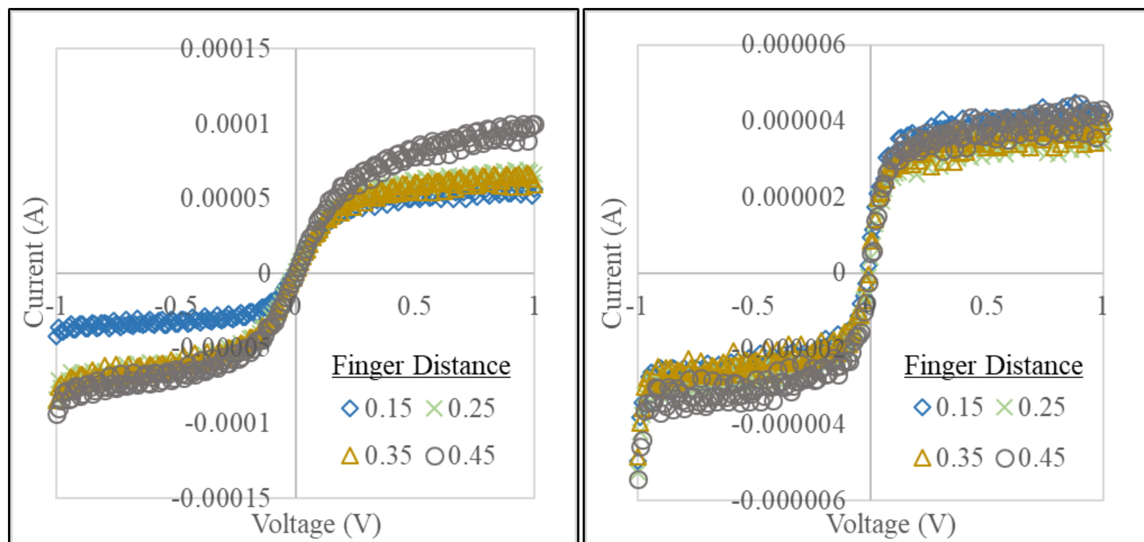

Figure 36: I-V characteristic for the samples with 6/40 (right) and 6/80 (left) as deposited

It is observable comparing Fig.36 with Fig.27 that the number of cycles of ALD obviously affects to the result obtained. However, it is also observable that even though the results are different, none of them allows conductance of electricity. In addition, after some anneals performed the results were even worse.

On the other hand, the results obtained were expected as the samples do not have phosphoric diffusion which gives us other example of the necessity of having a diffusion. Consequently, TLM technique was directly not performed over this samples and were discarded in first instance.

Moreover, it is observable comparing both plots on Fig.35 that the stronger is the buffer (6/80), the better are the results which is the reason for taking the weakest sample for work. (Remember that if we obtain a good characteristic with 6/20, consequently the 6/80 should be even better.) The following steps of the study with 6/20 can be found in section 4.2.2 as it is explained previously.

As a conclusion, more studies should be performed changing the buffer to know the behavior of the buffer and improve its characteristics because the results obtained may be promising for future investigations.

Glossary

ETL: Electron Transport Layer

ITO: Indium Tin Oxide

Ag: Argentum (Silver)

n^+: Doped with n impurities

c-Si: Crystalline silicon

TCO: Transparent Conductive Oxide

TLM: Transfer Length Method / Transfer Length Measurements / Transmission Line Measurement

SiO_2: Silicon Oxide

HF: Hydrofluoric acid

RCA: Radio Corporation of America

H_2O: Water

H_2O_2: Hydrogen peroxide

NH_3: Ammonia

HCl: Hydrogen Chloride

R_{sh}: Sheet Resistance

ρ_c: Specific contact resistance

W: Width

d: Distance

R_c: Contact Resistance

L_T: Transfer Length

L_C: Contact Length

τ_{eff}: Effective carrier lifetime

τ_{bulk}: Bulk Carrier lifetime

S_{eff}: Effective swiftness of recombination

J_0: Recombination current density

N_A: Concentration of acceptor impurities

q: Charge of a single electron

ni: Intrinsical concentration of minorities

ALD: Atomic Layer Deposition

Al_2O_3: Aluminum Oxide

$Al_2(CH_3)_6$: Trimethylaluminum

I-V: Intensity - Voltage

H_2N_2: Forming gas

Ω/Sq: Ohms / Square